

**PROTEOMIC CHANGES INDUCED BY KNOCKDOWN OF STATHMIN
IN BT549 BREAST CANCER CELL LINES**

by

Yumin Song

B.S, Fudan University, 2006

Submitted to the Graduate Faculty of
School of Pharmacy in partial fulfillment
of the requirements for the degree of
Master of Science

University of Pittsburgh

2009

UNIVERSITY OF PITTSBURGH
SCHOOL OF PHARMACY

This thesis was presented

by

Yumin Song

It was defended on

April 20th, 2009

and approved by

Regis R. Vollmer, PhD, Professor

Song Li, MD, PhD, Associate Professor

Charles Sfeir, DDS, PhD, Associate Professor

Thesis Director: Billy W. Day, PhD, Professor

Copyright © by Yumin Song

2009

PROTEOMIC CHANGES INDUCED BY KNOCKDOWN OF STATHMIN IN BT549 BREAST CANCER CELL LINES

Yumin Song, BS

University of Pittsburgh, 2009

Breast cancer incidence in women in the United States is 1 in 8 (about 13%). In the U.S., breast cancer death rates are higher than any other cancer besides lung cancer [1], and more than 25% cancers are classified as breast cancer [2]. In 2008, an estimated 182,460 new cases of invasive, along with 67,770 of non-invasive (in situ), breast cancers were diagnosed in women in the U.S. About 40,480 women in the U.S. were projected to die in 2008 from breast cancer [3].

Paclitaxel (Taxol), a microtubule (MT) stabilizing agent, was originally noted to be useful against breast cancers [4]. Yet, like with many other cancer therapeutic agents, resistance to paclitaxel remains a significant problem in treating malignancies. One potential mechanism for the resistance observed is alterations in microtubule dynamics and altered binding of paclitaxel to its cellular target, the microtubule [5]. Stathmin is a highly conserved, 17kDa protein that functions as an important regulator of microtubule dynamics. Several studies have shown potential correlations between stathmin levels and resistance to paclitaxel.

The latest results from our collaborator Prof. Mary Ann Jordan at the University of California-Santa Barbara clearly show that reduction of the level of stathmin in BT549 cells increases their sensitivity to paclitaxel (vide infra). This reduction must obviously result in some changes in the affected cells' proteome, which delivers a signal of regulatory importance to the MT system; The

goal of the project was to detect and characterize the earliest proteomic changes, using 2-D DiGE and MALDI-TOF-MS, of BT549 breast cancer cell lines engineered with constitutively lowered stathmin levels. Two proteins, Protein Kinase C epsilon and Microtubule-Associate Protein 6, were identified to be expressed at lower levels with statistical significance, and potential mechanisms exist for those two proteins to interact with stathmin and/or microtubules are discussed. Based on this information, it is proposed that stathmin may play a role in certain integrating as well as diverse intracellular regulatory pathways. It is expected that this more detailed understanding of protein profile changes in these cells will allow for more rational decision-making in further research of the mechanisms leading to paclitaxel resistance.

TABLE OF CONTENTS

1	INTRODUCTION.....	1
1.1	Hypothesis and specific aims.....	2
1.2	Background.....	3
1.2.1	Microtubules have an important role in mitotic processes.....	3
1.2.2	Paclitaxel: mechanisms of anti-cancer action and drug-resistance.....	4
1.2.3	Overexpression of stathmin in paclitaxel resistance.....	7
2	PRELIMINARY DATA	8
2.1	Cell culture and reagents.....	8
2.2	Results and discussion.....	9
3	RESEARCH METHODS AND RESULTS.....	11
3.1	Proteome change analysis using traditional 2D GEL electrophoresis.....	11
3.1.1	Experimental section.....	11
3.1.2	Results and discussion.....	17
3.2	Proteome change analysis using Zoom fractionated 2D electrophoresis with Cy-dye label.....	24
3.2.1	Experimental section.....	24
3.2.2	Results and discussion.....	29
	BIBLIOGRAPHY.....	43

LIST OF TABLE

Table 1. Typical workflow for proteomic experiments.....	2
Table 2. Proteins identified with significant score using MASCOT database search.....	42

LIST OF FIGURES

Figure 1. Illustration of microtubule structure and microtubule dynamics.....	4
Figure 2. Chemical and 3D structure of paclitaxel.....	6
Figure 3. Structure of stathmin and its function as destabilizer.....	8
Figure 4. Stathmin mRNA and protein levels in BT549 transfectants	9
Figure 5. Stathmin knockdown cells are more sensitive to paclitaxel than their scrambled vector control line.....	10
Figure 6. 2D gel image analysis using Delta2D before and after warping.....	13
Figure 7. 2D gel image analysis using Delta2D ratio filters.....	13
Figure 8. Typical workflow for in-gel digestion using trypsin as cleavage enzyme.....	16
Figure 9. SyproRuby stained gel image acquired by fluorescence microscope (KDC & KD1)...	17
Figure 10. Spots picking list generated by Delta2D software (KDC & KD1).....	18
Figure 11. MALDI mass spectrum of BSA standard acquired by Voyager workstation.....	19
Figure 12. MALDI mass spectrum of KDC acquired by Voyager workstation.....	19
Figure 13. Illustration of ZOOM 2D protein fractionator.....	21
Figure 14. Schematic of DIGE analysis.....	22
Figure 15. Chemical structure of DIGE dyes (Cy3 & Cy5).....	22
Figure 16. Image of Cy3 labeled KDC control cell line & Cy5 labeled KD1 cell line acquired by Prometrix CCD camera.....	32

Figure 17. MALDI mass spectrum of Band 1 acquired by 4800 plus MALDI-TOF/TOF.....	33
Figure 18. MALDI mass spectrum of Band 2 acquired by 4800 plus MALDI-TOF/TOF.....	33
Figure 19. Identification of PKC epsilon by mascot database search of band 1 (Search 1).....	34
Figure 20. Identification of PKC epsilon by mascot database search of band 1 (Search 2).....	36
Figure 21. Identification of MAP6 by mascot database search of band 2 (Search 1).....	38
Figure 22. Identification of MAP6 by mascot database search of band 2 (Search 2)	40

1.0 INTRODUCTION

The word "proteome" is a blend of "protein" and "genome", which is considered to be the protein complement produced at a given timepoint by the genome [7][8]. In the past, mRNA analysis has been used to predict the possible proteins expressed from gene sequences; this has been found to rarely correlate with protein content [9][10]. It is now known that mRNA is not always translated into protein [11], and the amount of protein produced from a given amount of mRNA depends on gene regulation and on the current physiological stage of the cell cycle. Furthermore, the proteome is more complicated than the genome. A single gene can be expressed to give a number of different, albeit related proteins through several ways, e.g.: alternative splicing of the pre-messenger RNAs; attachment of carbohydrate residues to form glycoproteins; or addition of phosphate groups to some of the amino acids in the protein. Proteomics is the large-scale study of proteins, particularly their structure and function, which not only confirms the presence of the protein, but also provides a direct measure of the quantity present [12]. The overall objective of this project was to study the proteome changes of BT549 breast cell lines with their stathmin “knocked down” by constitutively expressed silencing RNA, with particular emphasis on the use of mass spectrometric technologies and electrophoretic separation methods. The typical workflow for proteomic experiments is shown below as Table 1:

1	Biological Question	6	Protein Excision
2	Biological Sample	7	Protein Digestion
3	Sample Preparation	8	MS/Protein ID
4	2-D Gel Separation	9	Global Bioinformatics
5	Imaging	10	Proteomic Discovery

Table 1. Typical workflow for proteomic experiments

1.1 HYPOTHESIS AND SPECIFIC AIMS

Like many other cancer therapeutic agents, paclitaxel suffers from the development of resistance in the tumors being treated. This remains a significant problem in treating malignancies. Stathmin has been considered to be a potential factor in paclitaxel resistance. One potential mechanism for the resistance observed is alterations in microtubule dynamics and altered binding of paclitaxel to its cellular target, the microtubule [5]. Stathmin is a highly conserved, 17kDa protein that is an important regulator of microtubule dynamics. Several studies have shown potential correlations between stathmin levels and resistance to paclitaxel.

In order to explore the hypothesis that the knockdown of stathmin will cause proteome changes via decreasing the disassembly (increase the stability) of microtubules and thereby enhance the ability of paclitaxel to stabilize the microtubules, the effects of manipulating stathmin levels on paclitaxel response in BT549 breast cancer cell lines were examined as were the potential molecular mechanisms of stathmin-related paclitaxel sensitivity by examining the early stage proteomic changes in paclitaxel-sensitive BT549 cell lines using proteomics tools. DiGE coupled with MALDI-TOF/TOF-MS were used to identify the protein characterizations.

1.2 BACKGROUND

1.2.1 Microtubules have an important role in mitotic processes

Microtubules, important components of the cytoskeleton, are built with dimers of α -tubulin and β -tubulin. As shown in Figure 1, they are straight, hollow cylinders whose walls are made up of a ring of "protofilaments"; usually they have a diameter of around 24 nm and the length can grow from several μm (in all eukaryotic cells) to mm (in axons of nerve cells). One important property of microtubules is their dynamic nature. Microtubules can grow by polymerization of tubulin dimers, which is powered by hydrolysis of GTP; they can also shrink by release of tubulin dimers, so-called depolymerization: this alternating flux of polymerization and depolymerization is called microtubule dynamics [13][14][15].

Microtubules are involved in many cellular processes like mitosis, cytokinesis and vesicular transport [16][17]. In interphase, microtubules are radially arrayed from the microtubule organizing center of the cell near the nucleus and are highly dynamic. When the S-phase is complete and the cell is ready to divide, microtubules first completely disassemble then reassemble to form the mitotic spindle, via which the chromosomes aligned as sister chromatid pairs in the center of the spindle are physically parted and moved to opposite spindle poles. At last, the cell divides from one to two (cytokinesis) and the gap between is sealed off by microtubules and motor proteins.

Clearly, it is important for cells to keep appropriate control of microtubules dynamics; if the dynamics is altered or regulated in the wrong way, the cell function and cell cycle will be affected accordingly.

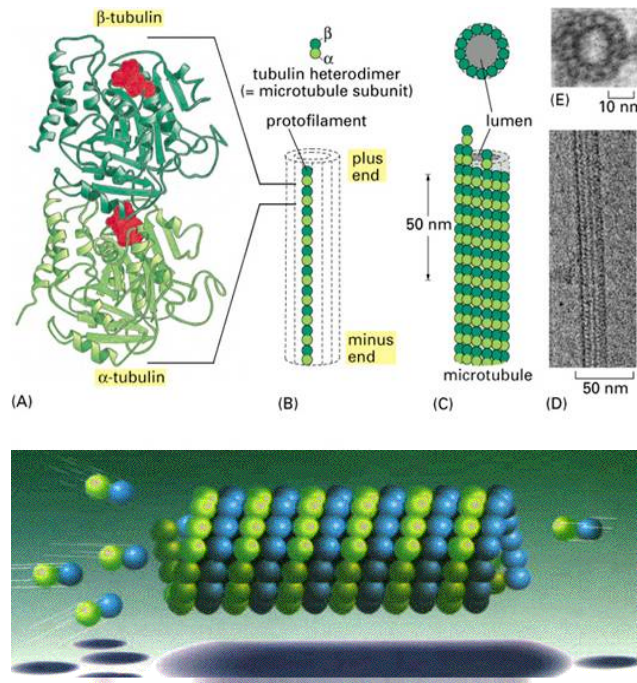


Figure 1. Illustration of microtubule structure and microtubule dynamics [excerpted from *Alberts B et al. Molecular Biology of The Cell, 4th Ed*]

1.2.2 Paclitaxel: mechanisms of anti-cancer action and drug-resistance

Cancer is essentially a disease of excess mitosis, and the microtubule cytoskeleton is an effective and validated target for cancer chemotherapeutic drugs [5]. Paclitaxel is a mitotic inhibitor used in cancer treatment [4][18][19]. Its mechanism of action is exerted by direct interaction with microtubules. It was discovered in a National Cancer Institute program at the Research Triangle Institute in 1967 when Monroe E. Wall and Mansukh C. Wani isolated it from the bark of the

Pacific yew tree, *Taxus brevifolia* and named it 'taxol' [20]. Fifteen years later, Susan Horwitz discovered its mechanism of microtubule binding and stabilization. Since discovery of semi-synthetic routes to its preparation and clinical introduction, and due to its ability to inhibit the tumor growth in some situations, paclitaxel has been applied in several clinical scenarios. For example, it now can be used for non-small cell lung cancer, first- and second-line treatment of ovarian cancer, and advanced breast cancer [21][22]. The chemical and 3D structure of paclitaxel is shown in Figure 2.

As for its mechanism of action, paclitaxel hyperstabilizes microtubule structure by specifically binding to β -tubulin. The microtubule/paclitaxel complexes lose the ability to disassemble, which alters microtubule dynamics and thus inhibits the process of cell division. In fact, some normal cells are also affected by paclitaxel treatment, but since it is the dividing cells that are most affected and cancer cells appear to have more dynamic tubulin than even the few types of rapidly dividing normal cells in the body (e.g., intestinal lining, bone marrow cells and hair follicles), it is the cancer cells that are most sensitive to paclitaxel. Interestingly, another normal cell that is often affected by paclitaxel is endothelial cells, but only those that are involved in neovascularization. Hence, paclitaxel also exerts antiangiogenic action against solid tumors [5]. Although paclitaxel has been demonstrated to have antitumor activity against several cancers, the emergence of resistance is a major limitation to its complete success. Chemotherapeutic failure may be related either to the tumor being inherently resistant to the drug and/or to the acquisition of resistance during treatment [5].

Drug resistance is often a multifactorial process that may originate through a series of modifications. In the case of paclitaxel, several potential mechanisms can be proposed to account for the resistance observed in human tumors and tumor cell lines. These include 1) overexpression of the multidrug transporter P-glycoprotein [23]. Paclitaxel administration restores expression of P-gp to high levels in blood and bone marrow of dogs transfected with an MDR1 retroviral vector. PCR analysis of DNA from peripheral blood confirmed that the retroviral cDNA is increased after paclitaxel treatment. 2) Altered metabolism of the drug, and decreased sensitivity to death-inducing stimuli [24]. Although paclitaxel causes increases in tubulin polymer mass and stabilizes microtubules, higher concentrations of paclitaxel are required to cause in resistant cells an increase in the total microtubule polymer mass than are required to inhibit microtubule function. While considering its mechanism of action, the most likely mechanisms of paclitaxel resistance should rely on altered microtubule dynamics and the binding of paclitaxel to the microtubule [5].

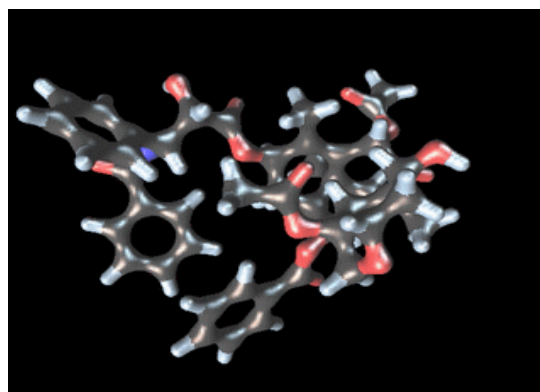
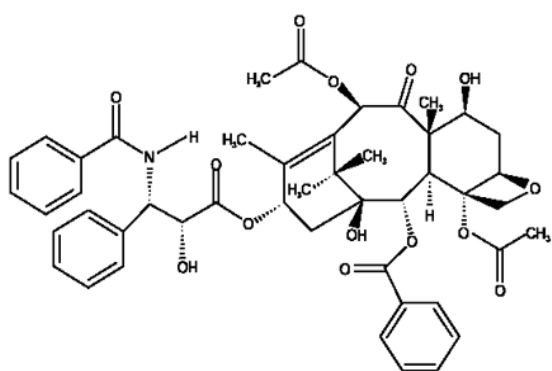


Figure 2. Chemical and 3D structure of paclitaxel [obtained from FDA document *ABRAXANE for Injectable Suspension, Version: Jan 7, 2005*]

1.2.3 Overexpression of stathmin in paclitaxel resistance

“Proteins that regulate microtubule dynamics by interacting with tubulin dimers or polymerized microtubules clearly have the potential to modulate the sensitivity of a cell towards Taxol” [5]. Stathmin, a 17kDa cytoplasmic phosphoprotein, represents one such protein that regulates the dynamics of cellular microtubules. It can interact with two α,β -tubulin heterodimers to form a tight complex, called the T2S complex (as shown in Figure 3), which prevents the tubulin to form microtubule and thus alter the microtubule dynamics (This destabilizing activity is regulated by phosphorylation, and is lost when stathmin is fully phosphorylated) [25][26][27]. Here, in contrast to paclitaxel, stathmin acts as a microtubule destabilizer.

Much work shows potential correlations between stathmin and paclitaxel resistance. Larsson et al. found that stathmin inhibits paclitaxel-induced polymerization of tubulin in vitro [28]. By generating two distinct classes of stathmin mutants, they found that both types of mutation result in stathmin with a limited decrease in tubulin complex formation. Their results also indicate that stathmin-tubulin contact involves structural motifs that deliver a signal of regulatory importance to the MT system. Other findings include the upregulation of stathmin mRNA and protein levels in tumor or paclitaxel resistant cell lines. Stathmin mRNA levels are upregulated in various carcinomas [29][30][31][32][33]. In fact, the name originally given to stathmin was Op-18 (oncoprotein of 18 kDa). The latest results from Mary Ann Jordan’s lab at the University of California-Santa Barbara clearly show that induced downregulation of stathmin increases the sensitivity to paclitaxel in BT549 cells. Together, these data indicate that the expression levels of

stathmin in cancer cells could be related the cells' sensitivity to paclitaxel; i.e, high level of stathmin would oppose the microtubule-stabilizing effect of paclitaxel.

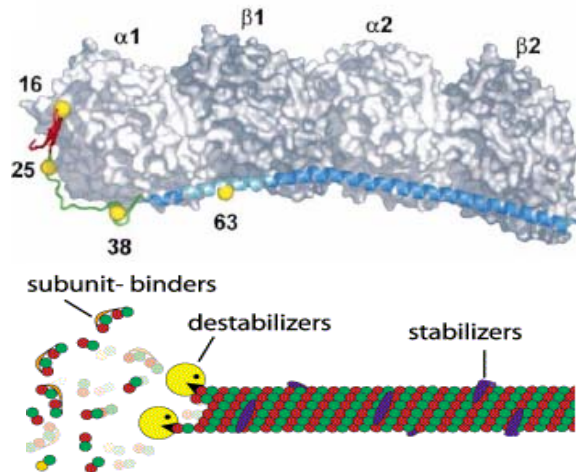


Figure 3. Structure of stathmin and its function as destabilizer [excerpted from *Honnappa et al, JBC 2006*]

2. PRELIMINARY DATA

2.1 Cell culture and reagents

BT549 breast cancer cell lines with stably-altered in terms of stathmin expression level were obtained from Prof. Mary Ann Jordan. These were generated by stable transfection using vectors containing shRNA targeting stathmin in the downstream of the RNA polymerase III (U6) promoter (stathmin knock-down cell lines; KD1 or KD2). The control cells were transfected with the vectors expressing scrambled RNA in the downstream of U6 promoter (stathmin knock-down control; KDc) using SuperFect Transfection Reagent (Qiagen Inc. Valencia, CA) by following manufactures instruction. The human U6 promoter drives RNA Polymerase III transcription for generation of shRNA transcripts and those vectors were used to provide efficient, long-term suppression of stathmin gene in cultured BT549 cells. Cells were maintained in RPMI-1640

medium (Sigma-Aldrich, St. Louis, MO) containing 0.2 mg/ml G418 (BioWhittaker, Walkersville, MD), supplemented with 10% fetal bovine serum (Hyclone, Logan, UT) and 0.1% penicillin/streptomycin at 37°C in a humidified 5% CO₂ environment. Paclitaxel was dissolved in DMSO (dimethylsulfoxide) at 10 mM and stored at –80°C as stock solutions.

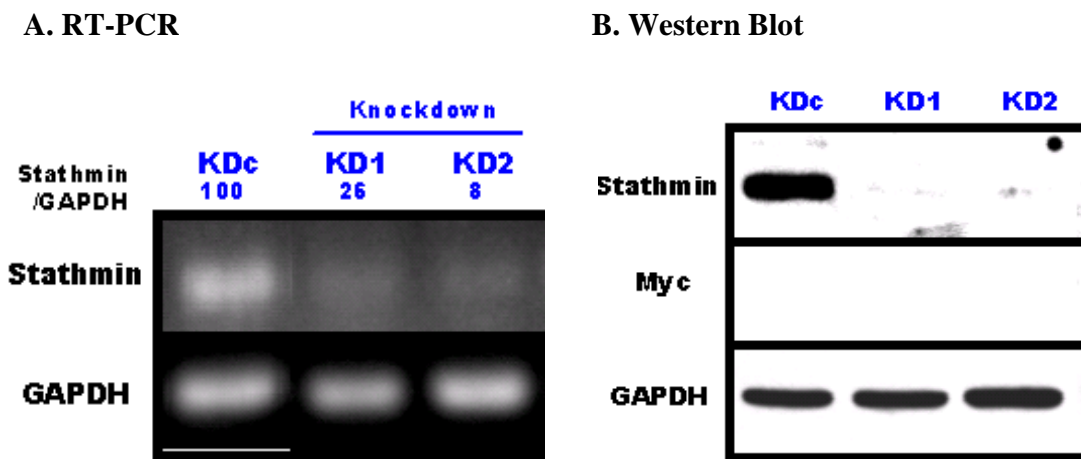


Figure 4. Stathmin mRNA and protein levels in BT549 transfectants [*courtesy provided by Prof. Mary Ann Jordan*]

KDc: knock-down control, KD1 & 2: knock-down lines

A. mRNA expression levels by RT-PCR. B. Protein expression levels by Western Blots.

2.2 Results and discussion

As shown in Figure 4, stathmin mRNA levels as determined by RT-PCR in KD cell lines were largely downregulated as compared to their KDc control (scrambled vector) cell lines. (KD1 and KD2 levels were 26 % and 8 % of KDc, respectively) Stathmin protein levels were also clearly decreased in cell lines.

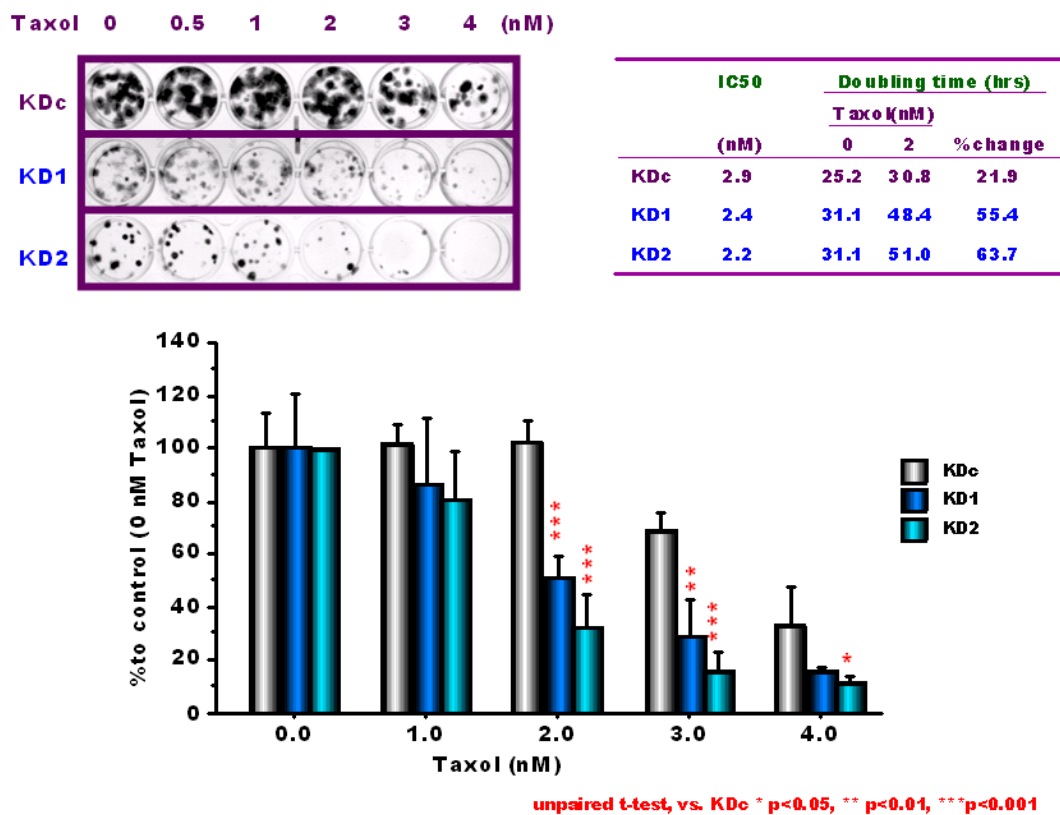


Figure 5. Stathmin knockdown cells are more sensitive to paclitaxel than their scrambled vector control line

[courtesy provided by Prof. Mary Ann Jordan]

The effects of paclitaxel on the proliferation of stathmin knockdown cell lines were examined also compared to their parental controls. As shown in Figure 5, paclitaxel at > 2.0 nM suppressed the proliferation of all of the cell lines investigated in a concentration dependent manner. The KD cell lines were more sensitive to paclitaxel. At 2 nM, paclitaxel induced a stronger suppression of cell proliferation in the stathmin knock-down cell lines (KD1; 46% and KD2; 48 %) as compared to their scrambled vehicle control (KDc; 32 %). These data suggest that stathmin might be an important factor in the regulation of cell growth, and it might directly influence the resistance to the effects of paclitaxel on cell proliferation.

3.0 RESEARCH METHODS AND RESULTS

3.1 PROTEOME CHANGE ANALYSIS USING TRADITIONAL 2D GEL ELECTROPHORESIS

3.1.1 Experimental section

Cell culture and cell lysis

Three cell lines, BT549 breast cancer cells stably infected with vectors encoding silencing RNA for stathmin (KD1 and KD2) and one encoding a scrambled vector (KDc), were obtained from Prof. Mary Ann Jordan and grown in RPMI-1640 with G418. Trypsinized cells were washed with cold Hanks balanced salts solution. After pelleting of cells by centrifugation, lysates were prepared in 10mM HEPES, pH 8.0, containing 6M urea, 4% CHAPS, 2M thiourea and 25mM dithiothreitol (DTT). The cell lysates then were centrifuged at 4 °C, 15,000xg for 15 min. Protein content was estimated using the BioRad procedure. An aliquot was treated with 4 volumes of ice-cold acetone overnight to precipitate (typically ~100 µg of) protein. After centrifuging, the acetone was removed and the pellet was dried, then dissolved at 100µg/100 µL of lysing buffer and stored at -80 °C until use.

2D gel electrophoresis

The protein solution (100 µg/100 µL) was first mixed with 150 µL of rehydration buffer containing 7M urea, 2M thiourea, 2% CHAPS, 50mM DTT and 4 µL of ampholyte mixture (BioRad). After mixing and quick centrifugation, the protein mixture was carefully layered onto a 17 cm IPG strip (pH 3-10 NL (non-linear); BioRad) in a tray (BioRad) onto which the IPG strip was placed. The strip then was covered with mineral oil. Isoelectric focusing (IEF) was done using a PROTEAN IEF cell (BioRad) at active rehydration mode for 60000V-h overnight. The IPG strips then were washed in an equilibration buffer (50mM Tris, pH 8.6, containing 6M urea, 30% glycerol, 2% SDS, bromophenol blue and 10mg/ml DTT) for 15 min at room temperature. After rinsing the strip with Millipore water, sulfhydryl groups were alkylated by addition of 25mg/mL iodoacetamide (also in the equilibration buffer) for 15 min, followed by rinsing in Millipore water. The strips were then transferred to running buffer (25mM Tris, pH 8.3, containing 192mM glycine and 0.1% SDS). For the second dimension, the IPG strips were carefully placed onto a BioRad PROTEAN II, 8-16% Tris-HCl Ready Gel, and covered with BioRad overlay agarose. After the overlay agarose solidified (ca. 10 min), the gel unit was assembled and run at constant 2W for 18 h in the cold room.

Gel image and image analysis

The gels were washed with deionized water (3x, 20 min each wash) followed by fixing for 3 h (or overnight) in aqueous 10% methanol and 7% acetic acid, and subsequently stained with SyproRuby overnight. After destaining and rinsing with deionized water, the images of the gels submerged in deionized water were obtained with WinDige software (J. Minden, Carnegie-

Mellon University) using a custom-built instrument with a high-resolution, cooled Prometrix® CCD camera and appropriate excitation/emission filters at 30 sec exposure times.

Digital images were analyzed with the DECODON Delta2D program to identify a differential display and relative quantitation of the proteins. After morphing/warping (as shown in Figure 6) of images for comparison, fused images were generated and the protein spots on the gels considered of interest (as shown in Figure 7) were identified in a scatter plot. Each scatter plot was a graphical representation of the protein spots on the gel images. In such a plot, spots whose level increased were found in the upper left and those decreased are in the lower right.

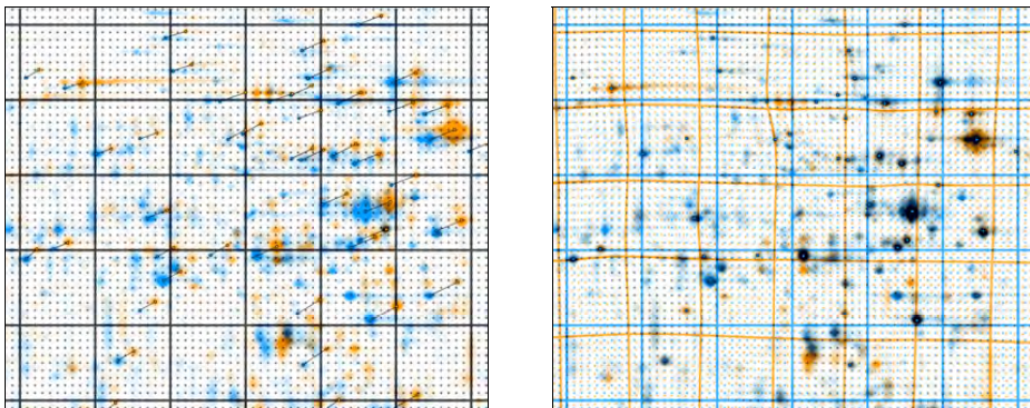


Figure 6. 2D gel image analysis using Delta2D before and after warping [excerpted from *Delta2D Manual*]

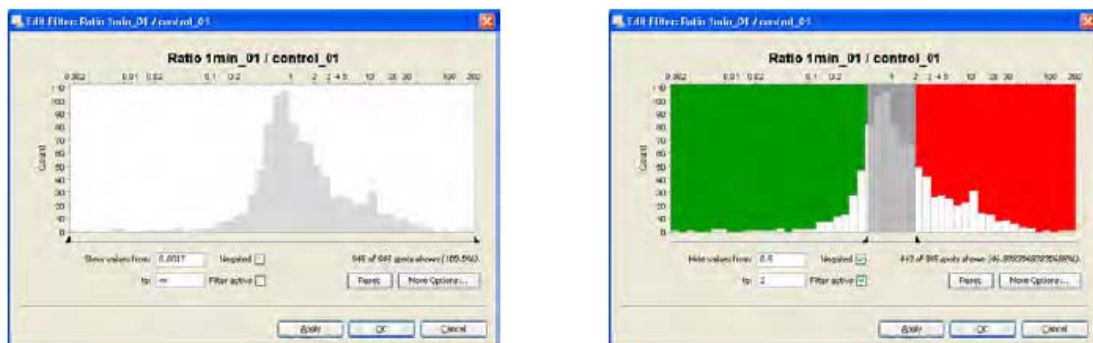


Figure 7. 2D gel image analysis using Delta2D ratio filters [excerpted from *Delta2D Manual*]

In-gel trypsin digestion

Proteins with volume changes > 2-fold were picked using robotic system on either the Minden scanner or a ProPic system (MANUFACTURER). The picked spots were then processed for in-gel digestion.

The protocol is based on the 10-year-old recipe by Shevchenko et al. [34], which has been optimized to increase the speed and sensitivity of analysis. A typical workflow for trypsin in-gel digestion is illustrated in Figure 8. Details are as follows. Protein spots of interest were excised. The gel pieces were transferred into a microcentrifuge tube and pelleted using a bench-top microcentrifuge. The spots were then processed for peptide mass fingerprinting and de novo sequencing: 500 μ L of neat acetonitrile was added to each spot and the tubes were incubated for 10 min until gel pieces shrank (became opaque). The gel pieces were pelleted by centrifugation and all liquid was removed. An aliquot 30–50 μ L of tris (2-Carboxyethyl) phosphine hydrochloride (TCEP) solution was added to completely cover gel pieces, which were then incubated for 30 min at 56 °C in a thermostatted chamber. The tubes were cooled to room temperature (ca. 22 °C) and 500 μ L of acetonitrile was added. The tubes were incubated for 10 min and then all liquid was removed. An aliquot (30–50 μ L) of iodoacetamide (IAC) solution (a volume sufficient to cover the gel pieces) was added and the tubes were incubated for 20 min at room temperature in the dark. Gel pieces were shrunk with acetonitrile and all liquid was removed.

The gel pieces were saturated with trypsin by adding enough trypsin buffer (50 mM ammonium bicarbonate, pH 7.8, containing sequencing grade porcine trypsin) to cover the dry gel pieces and

cooling in an ice bucket (to allow swelling but to decrease the amount of trypsin self-digestion). After 30 min, a check was made to insure all solution was absorbed and more trypsin buffer was added, if necessary. The gel pieces were allowed to sit for another 90 min to insure saturation with trypsin, and then an additional 10–20 μL of ammonium bicarbonate buffer was added to cover the gel pieces and keep them wet during enzymatic cleavage.

Digestion: Tubes with gel pieces were placed into a thermostatted chamber and incubated overnight at 37 °C. An aliquot was withdrawn from the digest for the protein identification by MALDI-TOF-MS peptide mass fingerprinting. Tubes were chilled to room temperature, the gel pieces were spun down using a microcentrifuge and 1–1.5 μL aliquots of the supernatant were directly withdrawn from the digest without further extracting the gel pieces. As the typical volume of the digestion buffer is approximately 50 μL this leaves ample peptide material for the subsequent MS/MS analysis, if required.

Peptide digestion products were extracted by adding 100 μL of extraction buffer (1:2 (v/v) 5% formic acid/acetonitrile) to each tube and incubation for 15 min at 37 °C in a shaker. The residual was dried down in a vacuum centrifuge and stored at –20 °C as a contingency.

and/or ProFound (http://prowl.rockefeller.edu/profound_bin/WebProFound.exe).

3.1.2 Results and discussion

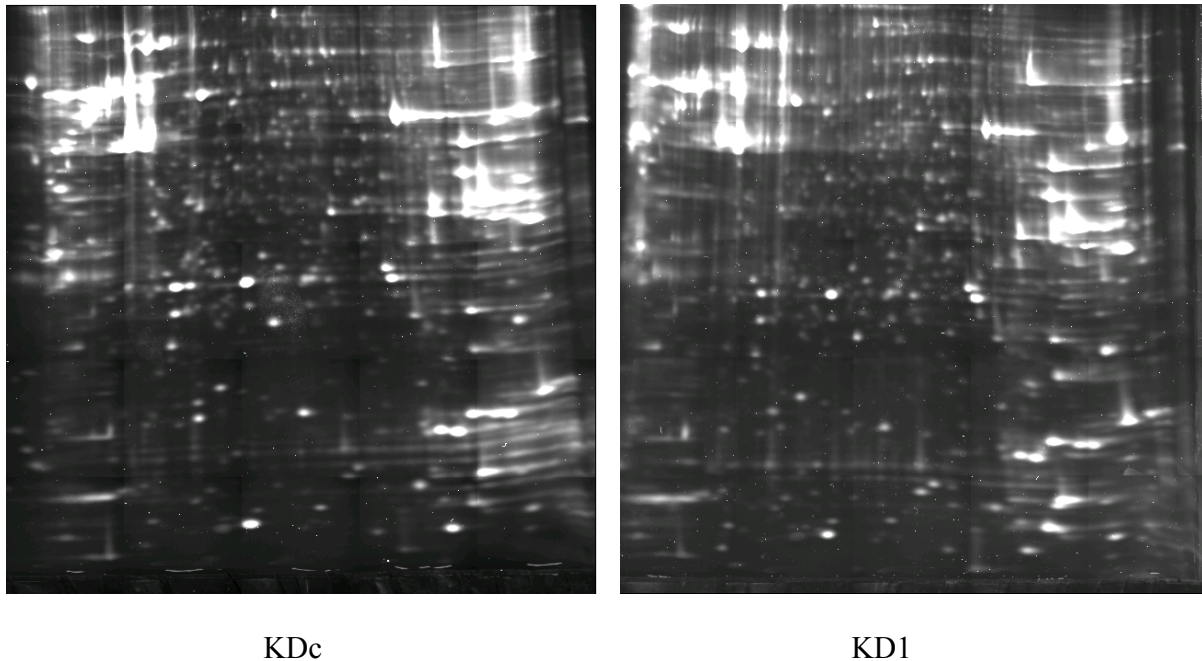


Figure 9. SyproRuby stained gel image acquired by fluorescence microscope (KDc & KD1)

Shown in Figure. 9 are two fluorescent images of KDc and KD1, of which several hundreds of proteins were separated and visualized. After analyzing the images with Delta 2D software [38], a picking list including about 300 spots of interest was generated. Most of them had volume changes over 2-fold. The picking lists are shown graphically in Figure 10.

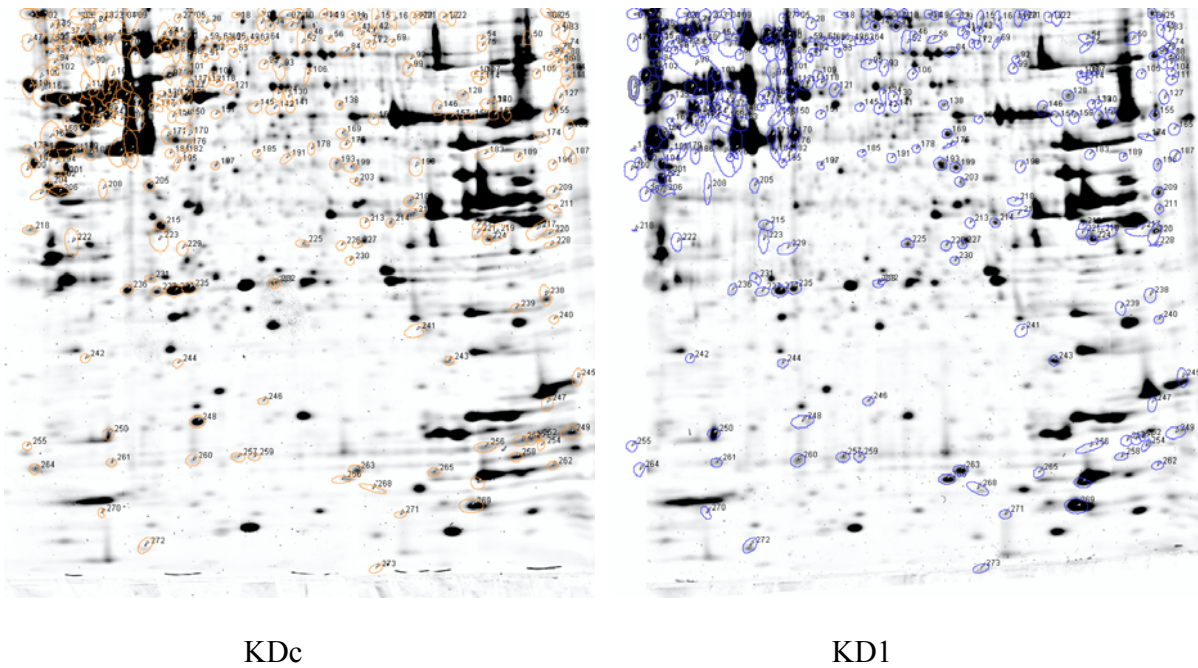


Figure 10. Spots picking list generated by Delta2D software (KDC & KD1)

Due to the high workload involved in spot picking, two robotic systems, a Propic system for picking and an Intavis liquid handling system with a Peltier unit for heating during enzymolysis were used. In spite of its high throughput and efficiency, shortcomings remained: the accuracy of picking not as high as needed; the digestion process was not as efficient as hoped; it was difficult to monitor and control the machines' operation during running; and, the user interface on each instrument was not user-friendly.

Figure 11 shows a spectrum of a trypsin in-gel digest of bovine serum albumin (BSA) from the above workflow acquired on the Voyager MALDI-TOF-MS, which confirmed that the digestion process was acceptable and successful. Yet, the spectra obtained for the spots from the gels run on lysates of the cell lines (both KDC and KD1) were not satisfactory, which made it impossible to identify specific proteins/peptides (sample mass spectrum shown in Figure 12).

BSA-Voyager

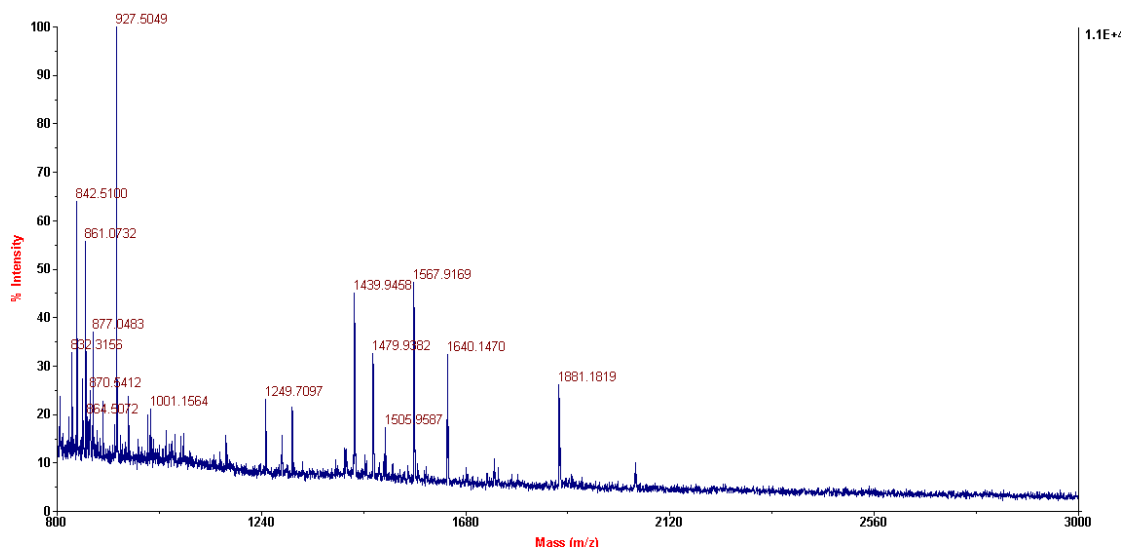


Figure 11. MALDI mass spectrum of BSA standard acquired by Voyager workstation

KDc-Voyager

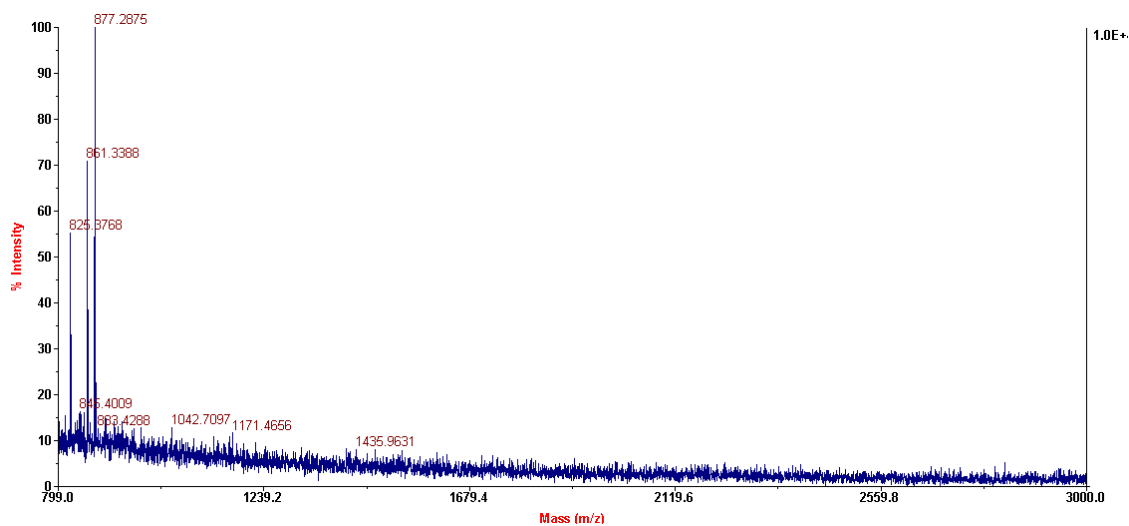


Figure 12. MALDI mass spectrum of KDc acquired by Voyager workstation

There might be several reasons for the inability to detect peptides/proteins and for unacceptable mass spectra: too little protein in the spots caused by poor protein solubility and protein aggregation [39]; spots without proteins due to spot picking robot displacement; the sensitivity of the mass spectrometer [40]; ion suppression [41][42]; and matrix quality [43]. These possible causes will be discussed below.

Efficient and reproducible sample preparation methods are key to successful 2-D gel electrophoresis. In the 2D gel images, several vertical streaks were observed, indicating a loss of solubility of protein at its pI during focusing and/or protein aggregation, especially hydrophobic proteins. One workaround is the total protein load applied to the isoelectric focusing strip could be decreased in an attempt to prevent the vertical streaks and improve the resolution of protein separation. In order to yield proteins of interest at detectable levels, however, removal of interfering abundant proteins or nonrelevant classes of proteins would be beneficial. Nucleic acids and other interfering molecules, e.g., lipids, could also be potential interfering factors. Thus, a new technique called ZOOM 2D protein fractionator (Figure 13), a solution-phase isoelectric focusing system was applied as the strategy to separate protein mixtures into reproducible and simplified fractions. The major benefits of this approach were its higher protein load capacity, complete solubilization and denaturation of the proteins, its maintenance of proteins in solution during IEF, sample fractionation, reduction and alkylation of disulfide bonds in proteins *prior* to IEF, and its enhanced capacity to prevent protein modifications and proteolysis.

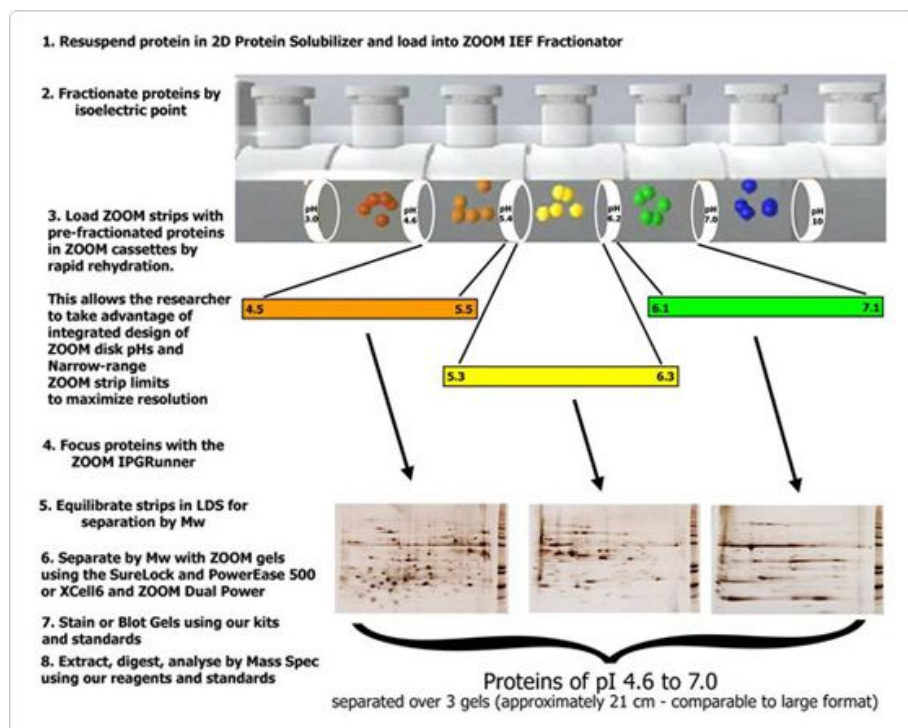


Figure 13. Illustration of ZOOM 2D protein fractionator [excerpted from *Zoom 2D fractionator manual*]

Traditional 2D electrophoresis requires considerable time and effort to analyze the resulting images due to inter-gel variation, so a new technique known as difference gel electrophoresis (DiGE), as shown in Figure 14-15, was employed instead of traditional 2D gel electrophoresis [44][45][46]. The proteins from the different sample types (KDc & KD1) were each labeled with one of two electrophilic dyes, PrCy3OSu or MeCy5OSu, then mixed and separated on the same gel where they could be directly compared. Because the versions of Cy3 and Cy5 are size and charge matched, the same labeled protein from different samples will migrate to the same position, regardless of the dye used. Also, fluorescence detection of these dyes is highly sensitive -- as little as 125 pg of protein can be detected. This provides better resolution and accuracy for future mass spectrum analysis.

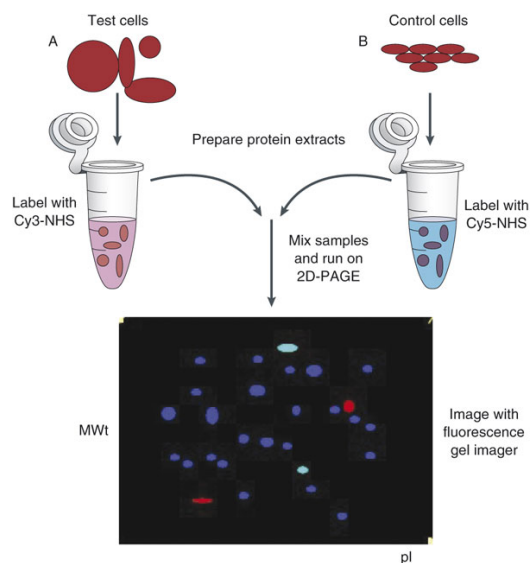


Figure 14. Schematic of DIGE analysis [excerpted from Jonathan S Minden et al. Nature Protocols 2006]

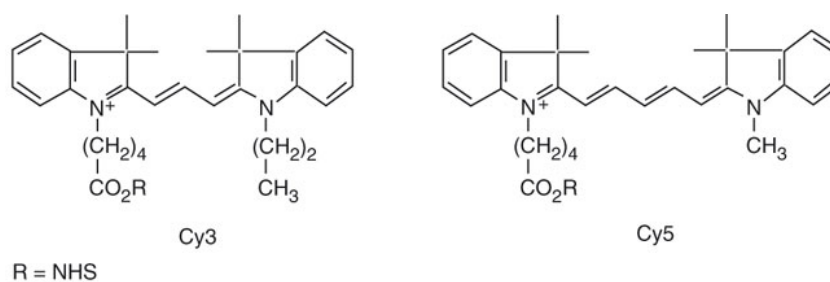


Figure 15. Chemical structure of DIGE dyes (Cy3 & Cy 5) [excerpted from Minden J. Biotechniques. 2007]

Due to the high throughput of data acquisition and analysis, the robotic gel picking, digestion and spotting were applied. Unfortunately, it turns out that the automated method did not provide as confident and stable results as expected. Thus, the staining method was switched to a reverse zinc stain and gel spots were manually removed.

Particularly, the interface (like low sample concentration, high ion/salt concentration, suppression of larger fragments) between protein digestion and mass spectrometric analysis had

a large influence on the overall quality and sensitivity of the analysis. It is ideal to concentrate, desalt, fractionate, and enrich protein/peptide samples prior to MS analysis. Sample cleanup could be achieved with the use of a ZipTip, which is a miniature reverse-phase column (solid phase extraction system) packed into a 10 μL pipet tip with a micro volume (approx 0.5 μL) bed of reversed-phase, ion exchange, or affinity chromatography medium fixed at its end without dead volume [47][48][49]. ZipTip-C18 tips can be used for purifying and concentrating femtomoles to picomoles of protein/peptide samples prior to analysis. After a process of wetting, binding, washing, recovered samples were contaminant free and eluted in 0.5–4 μL for direct transfer to a MALDI target.

In order to enhance the sensitivity of peptide detection, mass spectrometric determinations were made on an Applied Biosystems 4800 Plus MALDI-TOF/TOF-MS Analyzer. This tandem time-of-flight MS/MS system provided a higher level of protein coverage, throughput, and confidence in proteomic analysis. Its expanded dynamic range enabled higher confidence and sensitivity for identifying and quantifying low abundance proteins in complex matrices.

3.2 PROTEOME CHANGE ANALYSIS USING ZOOM FRACTIONATED 2D ELECTROPHORESIS WITH CY-DYE LABEL

3.2.1 Experimental section

Cell culture and cell lysates

The three cell lines (KDc, KD1 and KD2) were obtained from Prof. Mary Ann Jordan and grown in RPMI-1640 with G418. Trypsinised cells were washed with cold Hanks balanced salts solution. Lysis buffer was made using 2 μ L of 100X protease inhibitor cocktail, 8 units of benzonase and 148 μ L 40 mM tris base, mixed well and stored on ice until use. To 50 μ L of packed cells, 150 μ L of chilled lysis buffer was added. The lysate was then incubated for 30 min at room temperature. To this was added 25 μ L of 20 mM tris(2-carboxyethyl)phosphine hydrochloride (TCEP), 5.2 μ L of 50mM iodoacetamide (IAC) solution, 200 μ L of 20% (w/v) SDS and deionized water (to 1 mL) for reduction and alkylation. After centrifuging at 16,000 $\times g$ for 20 min at 4°C, the supernatant was transferred to sterile tubes in which cold acetone was added for protein precipitation. The precipitated pellet was washed with cold acetone, allowed to air-dry at room temperature, and resuspended in 1 mL of ZOOM® 2D Protein Solubilizer. Protein content was estimated using the BioRad procedure, aliquoted into smaller volumes and stored at -80° C.

Cy-dye labeling

Stock solutions (8.6 mM) of Cy-dyes (PrCy3-OSu and MeCy5-OSu) were prepared in the Day lab by dissolving the solid dyes separately in DMF and aliquoting into 10 μ L working solutions. The stock solution was stored at -80° C. Equal amounts of protein samples (lysates from KDc

control vs. stathmin knockdown KD1) were placed into tubes, mixed and spun briefly in a microcentrifuge. Each tube was treated with 1.0 μ L of PrCy3-OSu or MeCy5-OSu and incubated on ice in the dark for 20 min. Afterwards, 1.0 μ L of a hydroxysuccinide ester-quenching solution (5 M methylamine in 100 mM HEPES, pH 8.0) was added and the samples were incubated on ice in the dark for another 30 min. The paired tubes (Cy3 for KDc and Cy5 for KD1) were pooled and mixed well. An ampholyte solution (Bio-Lyte 3/10) was added to each tube and the contents were mixed well for rehydration.

ZOOM IEF Fraction

After labeling, the Cy-dye labeled lysates were diluted to 0.5 mg/mL for IEF fractionation with the ZOOM® IEF Fractionator. Diluted sample (1 mL) was prepared by mixing of the following: a) lysate prepared (51-64 μ L); b) 1.1X ZOOM® 2D Protein Solubilizer (909 μ L); c) ZOOM® Focusing Buffer, pH 3-7 (10 μ L); d) ZOOM® Focusing Buffer pH 7-12 (10 μ L); e) 2M dithiothreitol (DTT; 5 μ L); f) trace bromophenol blue dye. The volume was adjusted to 1.0 mL with deionized water. The diluted samples and running buffers were then loaded for IEF as described in the ZOOM® IEF Fractionator manual. Twenty to twenty-four fractions within narrow pH range were obtained and stored at -80° C until the next step of 2-D gel electrophoresis.

2-D Gel electrophoresis

NuPAGE® Novex 10% Tris-Acetate Midi gel was stored in the cold room until used. Samples were prepared by mixing 7 μ L fractions, 5 μ L NuPAGE® LDS Sample Buffer (4X), 2 μ L reducing agent (NuPAGE®) and 7 μ L deionized water to a final volume of 20 μ L. Each well was

loaded with 20 μ L of sample, and running conditions were as follows: Running buffer: 1X NuPAGE® SDS; Voltage: 200 V constant; Run time: 40 minutes.

2-D Gel image and analysis

The gels were fixed in water containing 40% methanol and 5% acetic acid for 1 h, then washed with deionized water 4-5 times. After rinsing, the images of the gels submerged in deionized water were obtained with WinDige software (J. Minden, Carnegie-Mellon University) using a custom-built instrument with a high-resolution, cooled Prometrix CCD camera and appropriate excitation/emission filters at 30 sec exposure times. Digital images were analyzed by manual comparison and/or with ImageJ, in which the intensity of gel bands was plotted by which interactive quantitation of those bands using simple interactive integration was made.

Gel visualization

The gel was also visualized by direct zinc-reverse staining. The gel was first rinsed briefly with dH₂O twice and submerged into fixing solution for 20 min, followed by washing twice in dH₂O for another 15 min with gentle shaking. The washed gel was incubated in 200-300 mL of 0.2M imidazole-SDS solution (13.6 g/L) for 15 min. After removing the imidazole-SDS solution, 200-300 mL of 0.3 M zinc sulfate was poured into the gel, with gentle agitation for 30-60 sec. Once the gel had stained satisfactorily (showing opaque on the blank gel background where protein was know to be absent), the zinc sulfate solution was quickly removed to prevent over-staining and the gel was stored in dH₂O for excising and in-gel digestion.

In-gel trypsin digestion

After visualizing with the direct zinc-reverse staining, protein bands of interest were excised for in-gel trypsin digestion. The protocol is based on the 10-year-old recipe by Shevchenko et al. [34], which has been optimized to increase the speed and sensitivity of analysis. Details are as follows. The gel pieces were transferred into a microcentrifuge tube and pelleted using a bench-top microcentrifuge. The spots were then processed for peptide mass fingerprinting and de novo sequencing: 500 μ L of neat acetonitrile was added to each spot and the tubes were incubated for 10 min until gel pieces shrank (became opaque). The gel pieces were pelleted by centrifugation and all liquid was removed. An aliquot 30–50 μ L of TCEP solution was added to completely cover gel pieces, which were then incubated for 30 min at 56 °C in a thermostatted chamber. The tubes were cooled to room temperature (ca. 22 °C) and 500 μ L of acetonitrile was added. The tubes were incubated for 10 min and then all liquid was removed. An aliquot (30–50 μ L) of iodoacetamide (IAC) solution (a volume sufficient to cover the gel pieces) was added and the tubes were incubated for 20 min at room temperature in the dark. Gel pieces were shrunk with acetonitrile and all liquid was removed.

The gel pieces were saturated with trypsin by adding enough trypsin buffer (50 mM ammonium bicarbonate, pH 7.8, containing sequencing grade porcine trypsin) to cover the dry gel pieces and cooling in an ice bucket (to allow swelling but to decrease the amount of trypsin self-digestion). After 30 min, a check was made to insure all solution was absorbed and more trypsin buffer was added, if necessary. The gel pieces were allowed to sit for another 90 min to insure saturation with trypsin, and then an additional 10–20 μ L of ammonium bicarbonate buffer was added to cover the gel pieces and keep them wet during enzymatic cleavage.

Digestion: Tubes with gel pieces were placed into a thermostatted chamber and incubated overnight at 37 °C. An aliquot was withdrawn from the digest for the protein identification by MALDI-TOF-MS peptide mass fingerprinting. Tubes were chilled to room temperature, the gel pieces were spun down using a microcentrifuge and 1–1.5 µL aliquots of the supernatant were directly withdrawn from the digest without further extracting the gel pieces. As the typical volume of the digestion buffer is approximately 50 µL this leaves ample peptide material for the subsequent MS/MS analysis, if required.

Peptide digestion products were extracted by adding 100 µL of extraction buffer (1:2 (v/v) 5% formic acid/acetonitrile) to each tube and incubation for 15 min at 37 °C in a shaker. The residual was dried down in a vacuum centrifuge and stored at –20 °C as a contingency.

Mass spectrometric analysis

MALDI-TOF/TOF-MS (ABI 4800 plus Proteomics Analyzer) was used to determine protein identities and analyze protein characteristics. Raw data was analyzed by manual comparison combined with MASCOT, ProteinProspector/MS-FIT and ProFound database searches. Processes were carried out as follows:

Each sample was reconstituted in 3 µL of 50% ACN with 0.1% TFA prior to MS analysis and 1µL was spotted on a MALDI target plate. After the samples dried, 0.5 µL of saturated matrix (10 mg/mL of α -cyano-4-hydroxycinnamic acid (CHCA) in 50% ACN with 0.1% TFA) was spotted on top of each sample and allowed to dry completely. The samples were then subjected to MALDI-TOF/TOF-MS analysis using 4800 Proteomics Analyzer (Applied Biosystem)

equipped with 4000 Explorer version 2.0. The instrument was operated in 2 kV reflector positive ion mode and calibrated with a calibration kit (Applied Biosystems) containing a mixture of standard peptides as a default calibration for spectra acquisition. Database searching was performed using online search engines, eg.

Mascot (http://www.matrixscience.com/search_form_select.html),

MS-Fit (<http://prospector.ucsf.edu/ucsfhtml4.0/msfit.htm>),

or Profound (http://prowl.rockefeller.edu/profound_bin/WebProFound.exe).

3.2.2 Results and discussion

Protein identification was based on the combined PMF and peptide sequence information acquired from MALDI-TOF-MS experiments. The results showed that two proteins, PKC epsilon and MAP6, were identified with statistical significance. (Figure 16-22)

PKC epsilon

Protein kinase C (PKC) is a family of serine- and threonine-specific protein kinases that can be activated by calcium and the second messenger diacylglycerol. PKC is thought to reside in the cytosol in an inactive conformation and translocate to the plasma membrane upon cell activation where it modifies various cellular functions through phosphorylation of target substrates. Findings suggest that phosphorylation of stathmin in REH6 cells could be in part mediated by PKC activation [50]. Work done by Prekeris et al. also discovered an actin-binding motif unique to the epsilon isoform of protein kinase C, and determined the interactions between protein kinase C-epsilon and filamentous actin [51].

The protein kinase C (PKC) family of proteins plays an important part in growth regulation and is implicated in tumorigenesis. Inhibition of the PKC epsilon pathway using a kinase-inactive, dominant-negative PKC epsilon, PKC epsilon (KR), led to a significant inhibition of proliferation of human NSCLC cells in a p53-independent manner. Other results reveal an important role for PKC epsilon signaling in lung cancer and suggest that one potential mechanism by which PKC epsilon exerts its oncogenic activity is through deregulation of the cell cycle via a p21/Cip1-dependent mechanism [52]. Furthermore, data from McJilton et al. shows that protein kinase C epsilon interacts with Bax and promotes survival of human prostate cancer cells, indicating that an association of PKC epsilon with Bax may neutralize apoptotic signals propagated through a mitochondrial death-signaling pathway [53]. The latest results clearly show that protein kinase C epsilon (PKC epsilon) protects breast cancer cells from tumor necrosis factor-alpha (TNF)-induced cell death [54].

In the present experiments, it appears that the downregulation of PKC induces a lowered level of phosphorylation of stathmin, which accordingly increases the functional (tubulin-sequestering) level, or at least the ratio of functional-to-phosphorylated stathmin, and compensates for the reduced amount of stathmin. This reaction might be a feedback regulation of potential PKC-stathmin pathway and of great importance to maintain the balance of microtubule dynamics. Considering its role in neutralizing apoptosis, the downregulation of PKC in KD1 group makes BT549 cells more likely to use normal cellular suicide mechanisms and thus, more sensitive to the treatment of paclitaxel, which is consistent with the previous observations in the present body of work.

MAP6

Proteins that interact with microtubules and/or free tubulin dimers also have the potential to regulate both catastrophe and rescue rates of microtubules [55]. The best characterized of these regulatory proteins are microtubule-associated proteins (MAPs), the majority of which stabilize microtubules by decreasing catastrophes and/or increasing rescues [56]. MAPs represent such proteins that regulate the dynamics of cellular microtubules [57][58]. They likely have the potential to modulate the sensitivity of a cell towards paclitaxel, and to make compensations when stathmin levels are altered.

The present work identified altered levels of a protein called MAP6, as known as microtubule-associated protein 6. MAP6 is a calmodulin-binding and -regulated protein that is involved in microtubule stabilization [59]. An alteration in the expression of MAP6 is predicted to modulate cancer cell sensitivity to microtubule-interacting drugs like paclitaxel. As for the downregulation of MAP6, one possible explanation is that the ability of MAP6 to stabilize microtubule could be lessened due to the reduced destabilizing function of stathmin; a decrease in MAP6 would be needed in order to retain the needed balance for microtubule dynamics.

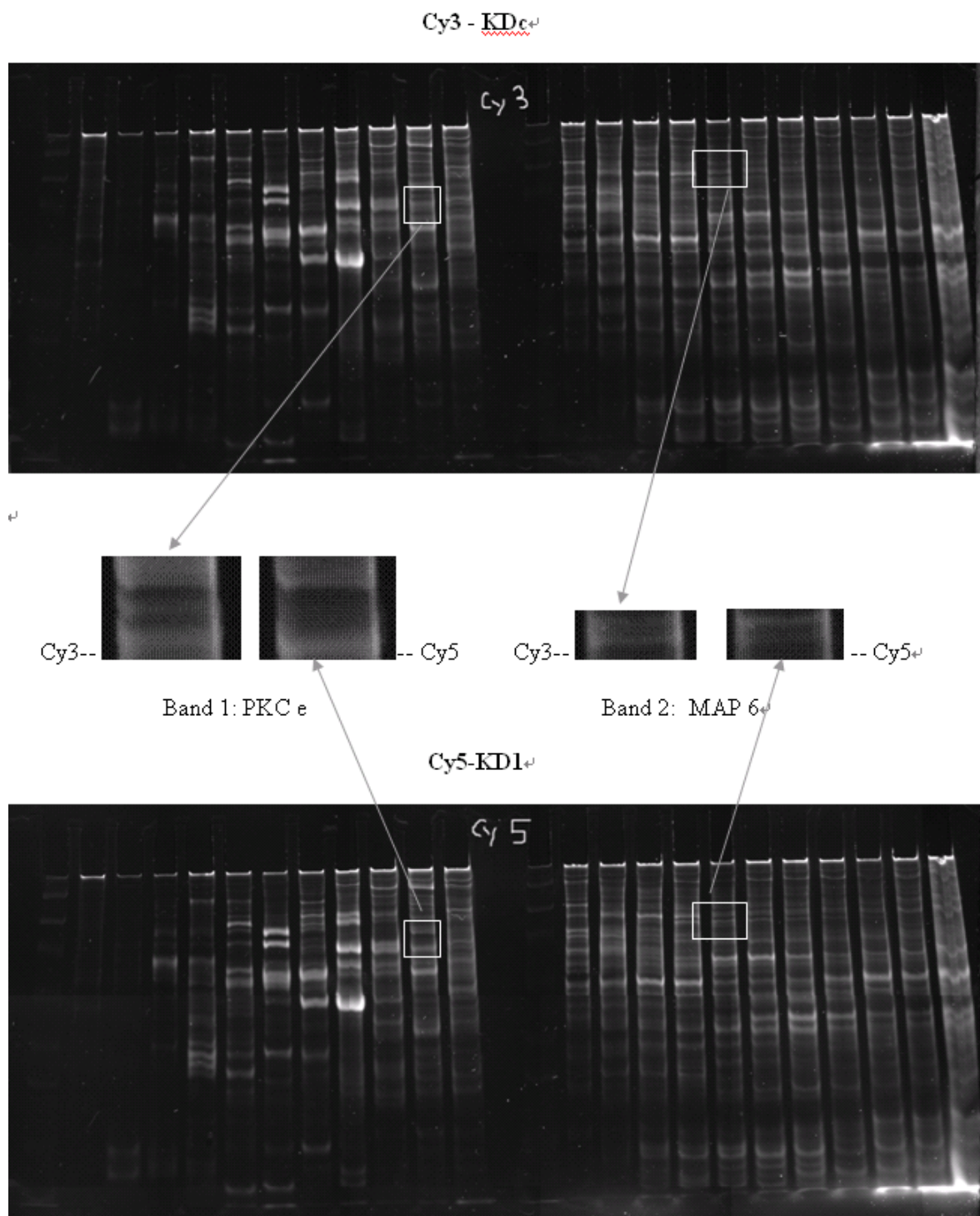


Figure 16. Image of Cy3 labeled KDc control cell line & Cy5 labeled KD1 cell line acquired by Prometrix CCD camera

PKC e - 4800

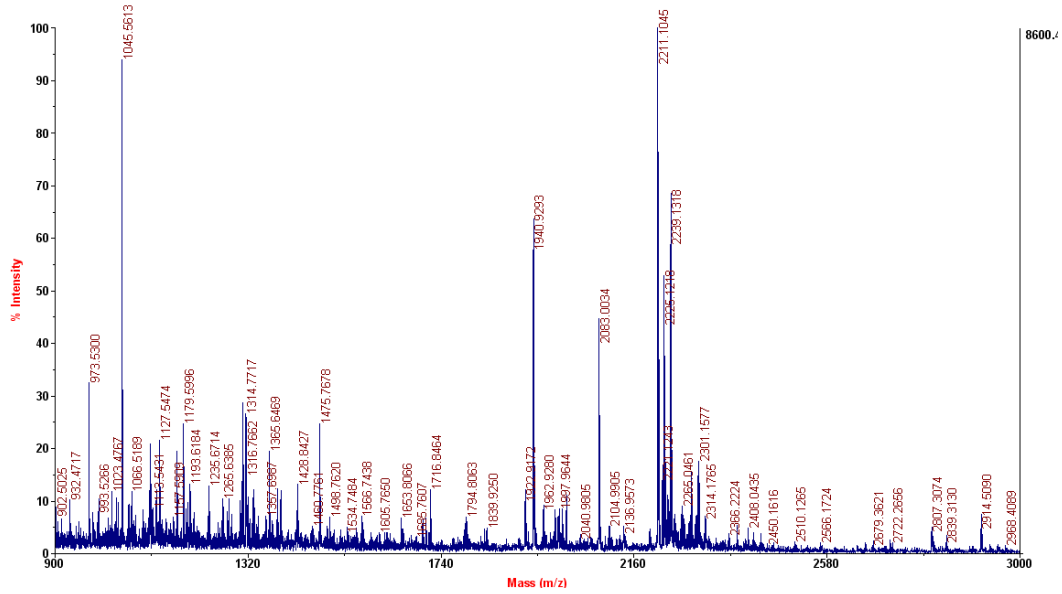


Figure 17. MALDI mass spectrum of Band 1 acquired by 4800 plus MALDI-TOF/TOF

MAP6 - 4800

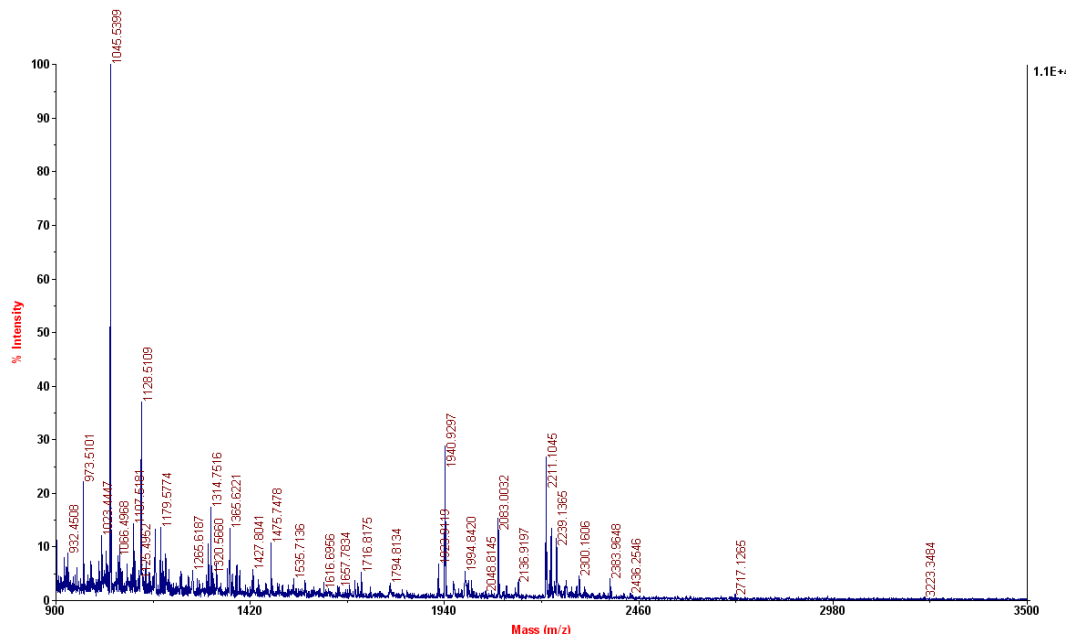


Figure 18. MALDI mass spectrum of Band 2 acquired by 4800 plus MALDI-TOF/TOF

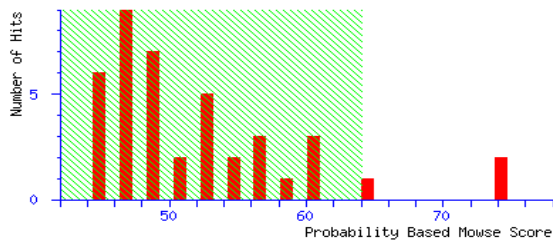
PKC epsilon (Search 1)

{MATRIX} *{SCIENCE}* Mascot Search Results

User : Yumin Song
Email : songyumin00@gmail.com
Search title :
Database : MSDB 20060831 (3239079 sequences; 1079594700 residues)
Taxonomy : Homo sapiens (human) (148148 sequences)
Timestamp : 26 Mar 2009 at 20:20:18 GMT
Top Score : 74 for **AAD04629**, AF110377 NID: - Homo sapiens

Probability Based Mowse Score

Protein score is $-10 \cdot \log(P)$, where P is the probability that the observed match is a random event.
Protein scores greater than 64 are significant ($p < 0.05$).



Concise Protein Summary Report

Format As Export Search Results [Help](#)
Significance threshold $p <$ Max. number of hits

- [AAD04629](#) Mass: 437304 Score: **74** Expect: 0.0056 Queries matched: 103
AF110377 NID: - Homo sapiens
[EAL23887](#) Mass: 434134 Score: **69** Expect: 0.019 Queries matched: 102
CH236956 NID: - Homo sapiens
[AAC27675](#) Mass: 236056 Score: 58 Expect: 0.24 Queries matched: 63
AC004991 NID: - Homo sapiens
[Q59FH1_HUMAN](#) Mass: 405555 Score: 57 Expect: 0.28 Queries matched: 99
Transformation/transcription domain-associated protein variant (Fragment).- Homo sapiens (Human).
- [S28942](#) Mass: 83620 Score: **74** Expect: 0.0063 Queries matched: 36
protein kinase C (EC 2.7.1.-) epsilon - human
- [Q3MN79_HUMAN](#) Mass: 142601 Score: 64 Expect: 0.066 Queries matched: 49
Centrosomal protein 1 (Fragment).- Homo sapiens (Human).
[Q5JVD1_HUMAN](#) Mass: 113695 Score: 46 Expect: 4 Queries matched: 38
Centrosomal protein 1.- Homo sapiens (Human).

Search Parameters

Type of search : Peptide Mass Fingerprint
Enzyme : Trypsin
Variable modifications : Carbamidomethyl (C), Oxidation (M)
Mass values : Monoisotopic
Protein Mass : Unrestricted
Peptide Mass Tolerance : ± 100 ppm
Peptide Charge State : 1+
Max Missed Cleavages : 1
Number of queries : 252

{MATRIX} Mascot Search Results

Protein View

Match to: S28942 Score: 74 Expect: 0.0063
protein kinase C (EC 2.7.1.-) epsilon - human

Nominal mass (M_n): 83620; Calculated pI value: 6.73

NCBI BLAST search of [S28942](#) against nr
Unformatted [sequence string](#) for pasting into other applications

Taxonomy: [Homo sapiens](#)

Links to retrieve other entries containing this sequence from NCBI Entrez:

[Q32MQ3_HUMAN](#) from [Homo sapiens](#)

[AAI09034](#) from [Homo sapiens](#)

[AAI09035](#) from [Homo sapiens](#)

[CAA46388](#) from [Homo sapiens](#)

[KPCE_HUMAN](#) from [Homo sapiens](#)

Variable modifications: Carbamidomethyl (C), Oxidation (M)

Cleavage by Trypsin: cuts C-term side of KR unless next residue is P

Number of mass values searched: 252

Number of mass values matched: 36

Sequence Coverage: 52%

Matched peptides shown in **Bold Red**

```

1  MVVFNGLLKI KICEAVSLKP TAWSLRHAVG PRPQTFLLDP YIALNVDDSR
51  IGQTATKQKT NSPAWHDEFV TDVNCGRKIE LAVFHDAPIG YDDFVANCTI
101 QFEELLQNGS RHFEDWIDLE PEGRVYVIID LSGSSGEAPK DNEERVFRER
151 MRPRKRQGVV RRRVHQVNGH KFMATYLRQP TYCSHCRDFI WGVIGKQGYQ
201 CQVCTCVVHK RCHELIITKC AGLKKQETPD QVGSQRFVSN MEHKFGIHNH
251 KVPTFCDHCG SLLWGLLRQG LQCKVCKMNV HRCETNVAP NCGVDARGIA
301 KVLADLGVTP DKITNSGQRR KKLIAGAESP QPASGSSPSE EDRSKSAPTS
351 PCDQEIKELE NNIRKALSFD NRGEHRAAS SPDGQLMSPG ENGEVRQGQA
401 KRLGLDEFNF IKVLGKGSFG KVMLAELK GK DEVYAVKVLK KDVI LQDDDV
451 DCTMTEKRIL ALARHPYLT QLYCCFQTKD RLEFFVMEYVN GGDLMFQIQR
501 SRKFDEPRSR FYAAEVTSL MFLHQHGVIY RDLKLDNILL DAEGHCKLAD
551 FGMCKE GILN GVTTITFCGT PDYIAPEILQ ELEYGPSVDW WALGVLMYEM
601 MAGQPFPEAD NEDDLFESIL HDDVLYPVWL SKEAVSILKA FMTKKNPHKRL
651 GCVASQNGED AIKQHFFFEK IDWVLEQKK IKPPFKPRIK TKRDVNNFDQ
701 DFTREEFVLT LVDEAIVKQI NQEEFKGFSY FGEDLMP
  
```

Show predicted peptides also

Sort Peptides By Residue Number Increasing Mass Decreasing Mass

Start	End	Observed	Mr(expt)	Mr(calc)	ppm	Miss	Sequence
1	11	1277.6381	1276.6908	1276.7577	-52	1	- MVVFNGLLKI.K I Oxidation (M)
27	57	3393.7695	3392.7623	3392.7841	-6	1	R.HAVGRPRPQTFLLDPYIALNVDDSRIGQTATK.Q
60	77	2104.9905	2103.9832	2103.9069	36	0	K.TNSPAWHDEFVTDVNCGR.K Carbamidomethyl (C)
60	78	2233.1125	2232.1053	2232.0018	46	1	K.TNSPAWHDEFVTDVNCGR.K I Carbamidomethyl (C)
125	145	2278.0823	2277.0750	2277.1124	-16	1	R.VVVIDLSGSSGEAPDNEER.V
163	171	1074.5265	1073.5192	1073.5843	-61	1	R.RVHQVNGH.K F
172	187	1992.9867	1991.9794	1991.8804	50	1	K.FMATYLRQPTYCSHCR.D Oxidation (M)
197	211	1922.9172	1921.9100	1921.8710	20	1	K.QQVCTCVVHGR.C 3 Carbamidomethyl (C)
212	224	1428.8437	1427.8364	1427.7628	51	1	R.CHELIITKCAQLK.K
212	224	1542.7488	1541.7415	1541.8058	-42	1	R.CHELIITKCAQLK.K 2 Carbamidomethyl (C)
225	236	1372.7178	1371.7105	1371.6743	26	1	K.QETFDQVGSQR.F
245	268	2890.4111	2889.4039	2889.4207	-6	1	K.FGIHNHVKVPTFCDHCGSLLWGLLR.Q 2 Carbamidomethyl (C)
269	277	1120.5720	1119.5647	1119.5529	11	1	R.QQLQCKVCK.M 2 Carbamidomethyl (C)
302	312	1127.5474	1126.5401	1126.6234	-74	0	K.VLADLGVTPDK.I
323	345	2300.1694	2299.1622	2299.0928	30	1	K.LIAGAESPQPASGSSPSEEDRSK.S
344	357	1490.7181	1489.7109	1489.7082	2	1	R.SKSAPTSPCDQEIK.E
346	357	1275.5309	1274.5236	1274.5813	-45	0	K.SAPTSPCDQEIK.E
346	357	1332.5486	1331.5413	1331.6027	-46	0	K.SAPTSPCDQEIK.E Carbamidomethyl (C)
373	396	2510.1265	2509.1192	2509.1252	-2	1	R.GEHRRAASPDGQLMSPGENGEVR.Q
403	412	1195.6071	1194.5998	1194.6285	-24	0	R.LGLDEFNFIK.V
441	457	1967.9216	1966.9144	1966.8864	14	1	K.KDVI LQDDDV DCTMTEK.R
441	457	2040.9805	2039.9732	2039.9028	35	1	K.KDVI LQDDDV DCTMTEK.R Carbamidomethyl (C); Oxidation (M)
442	457	1839.9250	1838.9178	1838.7914	69	0	K.DVI LQDDDV DCTMTEK.R
442	458	2011.9697	2010.9625	2010.8874	37	1	K.DVI LQDDDV DCTMTEK.R I Oxidation (M)
465	479	1929.8984	1928.8912	1928.9277	-19	1	R.RHPYLTQLYCCFQTK.D Carbamidomethyl (C)
465	479	1987.0698	1986.0625	1985.9492	57	1	R.RHPYLTQLYCCFQTK.D 2 Carbamidomethyl (C)
482	500	2323.0952	2322.0879	2322.1177	-13	0	R.LFFVMEYVNGDLMFQIQR.S Oxidation (M)
482	502	2566.1724	2565.1651	2565.2508	-33	1	R.LFFVMEYVNGDLMFQIQR.S K Oxidation (M)
535	547	1497.7667	1496.7594	1496.7293	20	0	K.LDNILLDAEGHCK.L Carbamidomethyl (C)
535	555	2306.1099	2305.1026	2305.0905	5	1	K.LDNILLDAEGHCKLADFGMCK.E
633	644	1337.6752	1336.6679	1336.7424	-56	1	K.EAVSILKAFMTK.N
640	648	1089.5176	1088.5103	1088.5437	-31	1	K.AFMTRKPK.R Oxidation (M)
650	663	1404.6653	1403.6580	1403.6715	-10	0	R.LGCVASQNGEDAIAK.Q
650	669	2246.1877	2245.1805	2245.0950	38	1	R.LGCVASQNGEDAIAKQHFFFEK.E Carbamidomethyl (C)
719	737	2279.0688	2278.0616	2278.0252	16	1	K.QINQEEFKGFSYFGEDLMP.-
727	737	1262.6090	1261.6017	1261.5325	55	0	K.GFSYFGEDLMP.-

No match to: 902.5025, 932.4717, 973.5300, 981.5933, 992.5745, 993.5266, 994.5459, 995.5610, 1023.4767, 1033.5164, 1037.5250,

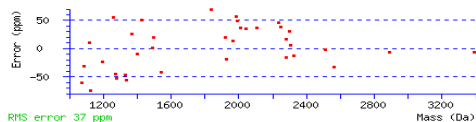


Figure 19. Identification of PKC epsilon by mascot database search of band 1 (Search 1)

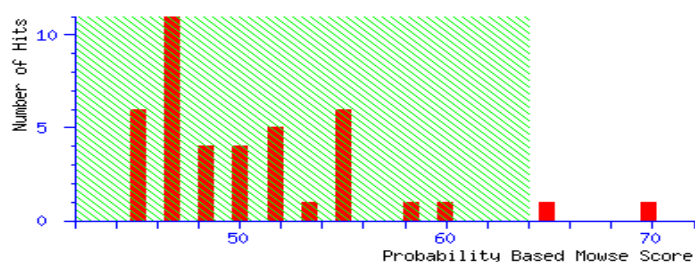
PKC epsilon (Search 2)

MATRIX *SCIENCE* Mascot Search Results

User : Yumin Song
Email : songyumin00@gmail.com
Search title :
Database : MSDB 20060831 (3239079 sequences; 1079594700 residues)
Taxonomy : Homo sapiens (human) (148148 sequences)
Timestamp : 26 Mar 2009 at 20:18:18 GMT
Top Score : 70 for **S28942**, protein kinase C (EC 2.7.1.-) epsilon - human

Probability Based Mowse Score

Protein score is $-10 \cdot \log(P)$, where P is the probability that the observed match is a random event. Protein scores greater than 64 are significant ($p < 0.05$).



Concise Protein Summary Report

[Help](#)

Significance threshold p< Max. number of hits

1.	S28942	Mass: 83620	Score: 70	Expect: 0.016	Queries matched: 37
protein kinase C (EC 2.7.1.-) epsilon - human					
2.	AAD04629	Mass: 437304	Score: 65	Expect: 0.046	Queries matched: 106
AF110377 NID: - Homo sapiens					
	EAL23887	Mass: 434134	Score: 58	Expect: 0.21	Queries matched: 105
CH236956 NID: - Homo sapiens					
	AAC27675	Mass: 236056	Score: 50	Expect: 1.7	Queries matched: 64
AC004991 NID: - Homo sapiens					
	Q59FH1_HUMAN	Mass: 405555	Score: 48	Expect: 2.1	Queries matched: 102
Transformation/transcription domain-associated protein variant (Fragment).- Homo sapiens (Human).					
3.	Q68CW5_HUMAN	Mass: 47453	Score: 59	Expect: 0.17	Queries matched: 25
Hypothetical protein DKFZp762A1314 (Fragment).- Homo sapiens (Human).					

Search Parameters

Type of search : Peptide Mass Fingerprint
Enzyme : Trypsin
Variable modifications : Carbamidomethyl (C), Oxidation (M)
Mass values : Monoisotopic
Protein Mass : Unrestricted
Peptide Mass Tolerance : ± 100 ppm
Peptide Charge State : 1+
Max Missed Cleavages : 1
Number of queries : 271

MATRIX Mascot Search Results

Protein View

Match to: S28942 Score: 70 Expect: 0.016
protein kinase C (EC 2.7.1.-) epsilon - human

Nominal mass (M₀): 83620; Calculated pI value: 6.73

NCBI BLAST search of [S28942](#) against nr
Unformatted [sequence string](#) for pasting into other applications

Taxonomy: [Homo sapiens](#)

Links to retrieve other entries containing this sequence from NCBI Entrez:

[Q32MQ3_HUMAN](#) from [Homo sapiens](#)
[AAI09034](#) from [Homo sapiens](#)
[AAI09035](#) from [Homo sapiens](#)
[CAA46386](#) from [Homo sapiens](#)
[KPCE_HUMAN](#) from [Homo sapiens](#)

Variable modifications: Carbamidomethyl (C), Oxidation (M)

Cleavage by Trypsin: cuts C-term side of KR unless next residue is P

Number of mass values searched: 271

Number of mass values matched: 37

Sequence Coverage: 54%

Matched peptides shown in **Bold Red**

```

1  MVVFNGLLKI KICEAVSLKP TAWSLRHAVG PRPQTFLLDP YIALNVDDSR
51  IQGTATKQKT NSPAWHDEFV TDVNGRRIE LAVFHDAPIG YDDFVANCTI
101 QFEELLQNGS RHFEDWIDE PEGRVYVIID LSGSSGEAPK DNEERVFRER
151 MRPRKRQGA VRRVHVQVNGH KFMATYLRQP TYCASHCRDFI WGVIGKQGYR
201 CQVCTCVVHK RCHELIITKC AGLKKQETPD QVGSQRFSVN MPHFKGIHNY
251 KVPVFCDHCG SLLWGLLRQ LQCKVCKMNV HRCETNVAP NCGVDARGIA
301 KVLADLGVT PDKITNSGQRR KCLIAGAESP QPASGSSPSE EDRSKSAPTS
351 PCQDEIKELE NNIRKALSFD NRGEHRAAS SPDGQLMSPG ENGEVRQGGQA
401 KRLGLDEFNF IKVLGKGSFPG KVMLAELK GK DEVYAVKVLK KDVILQDDDV
451 DCTMTEKRIL ALARKHPYLT QLYCCFQTKD RLFVMEYVN GGDLMFQIQR
501 SRKFDEPRSR FYAAEVTISAL MFLHQHGVYI RDLKLDNILL DAEGHCKLAD
551 FGMCKREGILN GVTTTTFCGT PDYIAPAILQ ELEYGPSVDW WALGVLMYEM
601 MAGQPFPEAD NEDDLFESIL HDDVLYPVWL SKEAVSILKA FMTKNPHKRL
651 GCVASQNGED AIKQHPFPKE IDVVLLEQKK IKPFPKRIK TKRDVNNFDQ
701 DFTREEPVLT LVDEAIVKQI NQEEFKGSYS FGEDLMP
    
```

Show predicted peptides also

Sort Peptides By Residue Number Increasing Mass Decreasing Mass

Start - End	Observed	Mr (expt)	Mr (calc)	ppm	Miss Sequence
1 - 11	1277.6981	1276.6908	1276.7577	-52	1 - MVVFNGLLKI.K.I Oxidation (M)
27 - 57	3393.7695	3392.7623	3392.7841	-6	1 R.HAVGERPQTFLLDPYIALNVDDSRIGQTATK.Q
60 - 77	2104.9905	2103.9832	2103.9069	36	0 K.TNSPAWHDEFVTDVNGR.K Carbamidomethyl (C)
60 - 78	2233.1125	2232.1053	2232.0018	46	1 K.TNSPAWHDEFVTDVNGR.K.I Carbamidomethyl (C)
125 - 145	2278.0823	2277.0750	2277.1124	-16	1 R.VYVILDLSSGSGEAPKDNEER.V
163 - 171	1074.5265	1073.5192	1073.5843	-61	1 R.RVHVQVNGHK.F
172 - 187	1992.9667	1991.9794	1991.8804	50	1 K.FMATYLRQPTCSHCR.D Oxidation (M)
197 - 211	1922.9172	1921.9100	1921.8710	20	1 K.QYQCQVCTCVVHKR.C 3 Carbamidomethyl (C)
212 - 224	1428.8427	1427.8354	1427.7628	51	1 R.CHELIITRCAGLK.K
212 - 224	1542.7488	1541.7415	1541.8058	-42	1 R.CHELIITRCAGLK.K 2 Carbamidomethyl (C)
225 - 236	1372.7178	1371.7105	1371.6743	26	1 K.QETPFDQVGSQR.F
245 - 268	2890.4111	2889.4039	2889.4207	-6	1 K.FGIHNYKVPVFCDHGSLWGLLR.Q 2 Carbamidomethyl (C)
269 - 277	1120.5720	1119.5647	1119.5529	11	1 R.QGLQCKVCK.M 2 Carbamidomethyl (C)
302 - 312	1127.5474	1126.5401	1126.6234	-74	0 K.VLADLGVTPEDE.I
323 - 345	2300.1694	2299.1622	2299.0928	30	1 K.LIAGAESPASGSSPSEEDRSK.S
344 - 357	1490.7181	1489.7109	1489.7082	2	1 R.SKSAPTSPCQDEIK.E
346 - 357	1275.5309	1274.5236	1274.5813	-45	0 K.SAPTSPCQDEIK.E
346 - 357	1332.5486	1331.5413	1331.6027	-46	0 K.SAPTSPCQDEIK.E Carbamidomethyl (C)
373 - 396	2510.1265	2509.1192	2509.1252	-2	1 R.GEEHRAASSPDGQLMSPGENGEVR.Q
403 - 412	1195.6071	1194.5998	1194.6285	-24	0 R.LGLDEFNF.K.V
413 - 421	892.5096	891.5024	891.5178	-17	1 K.VLKGKGSFPG.V
441 - 457	1967.9216	1966.9144	1966.8864	14	1 K.KDVILQDDVDVDCMTEK.R
441 - 457	2040.9805	2039.9732	2039.9028	35	1 K.KDVILQDDVDVDCMTEK.R Carbamidomethyl (C); Oxidation (M)
442 - 457	1839.9250	1838.9178	1838.7914	69	0 K.DVILQDDVDVDCMTEK.R
442 - 458	2011.9697	2010.9625	2010.8874	37	1 K.DVILQDDVDVDCMTEK.R.I Oxidation (M)
465 - 479	1929.8984	1928.8912	1928.9277	-19	1 R.KHPYLTQLYCCFQTK.D Carbamidomethyl (C)
465 - 479	1987.0698	1986.0625	1985.9492	57	1 R.KHPYLTQLYCCFQTK.D 2 Carbamidomethyl (C)
482 - 500	2323.0952	2322.0879	2322.1177	-13	0 R.LFFVMEYVNGDLMFQIQRS.S Oxidation (M)
482 - 502	2566.1724	2565.1651	2565.2508	-33	1 R.LFFVMEYVNGDLMFQIQRSR.K Oxidation (M)
535 - 547	1497.7667	1496.7594	1496.7293	20	0 K.LDNILLDAEGHCK.L Carbamidomethyl (C)
535 - 555	2306.1099	2305.1026	2305.0905	5	1 K.LDNILLDAEGHCKLADFGMCK.E
633 - 644	1337.6752	1336.6679	1336.7424	-56	1 K.EAVSILKAFMTK.N
640 - 648	1089.5176	1088.5103	1088.5437	-31	1 K.AFMTEKPHK.R Oxidation (M)
650 - 663	1404.6653	1403.6580	1403.6715	-10	0 R.LCVASQNGEDAIK.Q
650 - 669	2246.1877	2245.1805	2245.0950	38	1 R.LCVASQNGEDAIKQHPFK.E Carbamidomethyl (C)
719 - 737	2279.0688	2278.0616	2278.0252	16	1 K.QNQEERKGSYFGEDLMP.-
727 - 737	1262.6090	1261.6017	1261.5325	55	0 K.GFSYFGEDLMP.-

No match to: 806.4258, 807.3870, 825.0906, 827.4625, 840.4800, 842.5099, 847.4476, 850.4886, 856.5157, 861.0574, 864.4806, 866.4688,

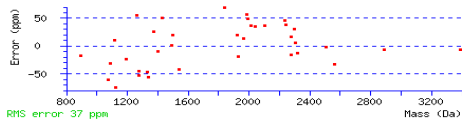


Figure 20. Identification of PKC epsilon by mascot database search of band 1 (Search 2)

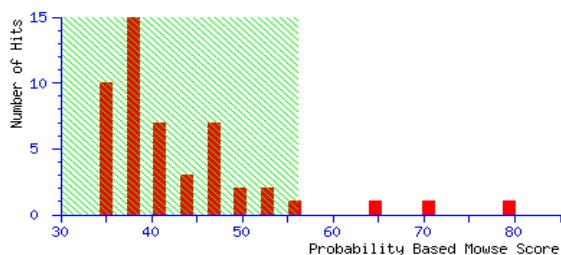
MAP6_HUMAN (Search 1)

{MATRIX} Mascot Search Results *{SCIENCE}*

User : Yumin Song
Email : songyumin00@gmail.com
Search title :
Database : SwissProt 56.9 (412525 sequences; 148809765 residues)
Taxonomy : Homo sapiens (human) (20402 sequences)
Timestamp : 26 Mar 2009 at 20:06:15 GMT
Top Score : 79 for **K2C1_HUMAN**, Keratin, type II cytoskeletal 1 OS=Homo sapiens GN=KRT1 PE=1 SV=5

Probability Based Mowse Score

Protein score is $-10 \cdot \log(P)$, where P is the probability that the observed match is a random event.
Protein scores greater than 56 are significant ($p < 0.05$).



Concise Protein Summary Report

Format As [Help](#)
Significance threshold $p <$ Max. number of hits

- [K2C1_HUMAN](#) Mass: 65978 Score: **79** Expect: 0.00023 Queries matched: 27
Keratin, type II cytoskeletal 1 OS=Homo sapiens GN=KRT1 PE=1 SV=5
- [MAP6_HUMAN](#) Mass: 86452 Score: **71** Expect: 0.0017 Queries matched: 28
Microtubule-associated protein 6 OS=Homo sapiens GN=MAP6 PE=1 SV=2
- [K22E_HUMAN](#) Mass: 65825 Score: **65** Expect: 0.0071 Queries matched: 23
Keratin, type II cytoskeletal 2 epidermal OS=Homo sapiens GN=KRT2 PE=1 SV=1

Search Parameters

Type of search : Peptide Mass Fingerprint
Enzyme : Trypsin
Variable modifications : Carbamidomethyl (C), Oxidation (M)
Mass values : Monoisotopic
Protein Mass : Unrestricted
Peptide Mass Tolerance : ± 80 ppm
Peptide Charge State : 1+
Max Missed Cleavages : 1
Number of queries : 188

MATRIX Mascot Search Results

Protein View

Match to: MAP6_HUMAN Score: 71 Expect: 0.0017
 Microtubule-associated protein 6 OS=Homo sapiens GN=MAP6 PE=1 SV=2

Nominal mass (M_r): 86452; Calculated pI value: 9.20
 NCBI BLAST search of [MAP6_HUMAN](#) against nr
 Unformatted [sequence string](#) for pasting into other applications

Taxonomy: [Homo sapiens](#)

Variable modifications: Carbamidomethyl (C), Oxidation (M)
 Cleavage by Trypsin: cuts C-term side of KR unless next residue is P
 Number of mass values searched: 188
 Number of mass values matched: 28
 Sequence Coverage: 38%

Matched peptides shown in **Bold Red**

```

1  MAWPCITRAC  CIARFWNQLD  KADIAVPLVF  TKYSEATEHP  GAPPQPPPQ
51  QQAQPALAPP  SARAVAIETQ  PAQGELDAVA  RATGPAPGPT  GEREPAAGFG
101 RSGPGPLGS  GSTSGPADSV  MRQDYRAWKV  QRPEPSCRPR  SEYQPSDAFF
151 ERETQYQKDF  RAWPLPRRGD  HPWIPKPVQI  SASASASAPI  LGAPKRRPQS
201 QERWFVQAAA  EAREQEAAPG  GAGGLAAGKA  SGADERDTRR  KAGPAWIVRR
251 AEGLGHEQTP  LPAAQAQVQA  TGPEAGRGRA  AADALNRQIR  EEVASAVSS
301 YRNEFRAWTD  IKPVKPIKAK  PQYKPDDKM  VHETSYSAQF  KGEASKPTTA
351 DNKVIDRRRI  RSLYSEFFKE  PPKVEKPSVQ  SSKPKTSAS  HKPTRKAKDK
401 QAVSGQAAKK  KSAEGPSTTK  PDDKEQSKEM  NNKLAEAKES  LAQPVSDSSK
451 TQGPVATEDH  KDQGSVVPGL  LKGQGPMVQE  PLKKQGSVVP  GPPKDLGPMI
501 PLPVKDQDHT  VEPLKNESP  VISAPVKDQG  PSVPVPPKNQ  SPMVPAKVKD
551 QGSVVPESLK  DQGPRIPEPV  KNQAPMVPAP  VKDEGPMVSA  SVKDQGPMVS
601 APVKDQGPIV  PAPVKGEGPI  VPAPVKDEGP  MVSAPIKDQD  PMVPEHPKDE
651 SAMATAPIKN  QGSMVSEPVK  NQGLVVSGPV  KDQDVVVPEH  AKVHDSAVVA
701 PVKNQGPVVP  ESVKNQDPIL  PVLVKDQGPT  VLQPPKNQRG  IVPELKNQV
751 PIVPVLKDQ  DPLVPVPAKD  QGPAVPEPLK  TQGPRDPQLP  TVSPLPRVMI
801 PTAPHTEYIE  SSP
  
```

Show predicted peptides also

Sort Peptides By Residue Number Increasing Mass Decreasing Mass

Start - End	Observed	Mr (expt)	Mr (calc)	ppm	Miss Sequence
1 - 8	993.4906	992.4833	992.4572	26	0 --.M A W P C I T R . A Oxidation (M)
1 - 8	1034.4630	1033.4557	1033.4837	-27	0 --.M A W P C I T R . A Carbamidomethyl (C)
1 - 14	1651.7560	1650.7487	1650.7615	-8	1 --.M A W P C I T R A C C I A R . F Carbamidomethyl (C)
2 - 14	1520.6843	1519.6768	1519.7210	-50	1 M. A W P C I T R A C C I A R . F Carbamidomethyl (C)
15 - 32	2104.9756	2103.9683	2104.1357	-80	1 R. P W N Q L D K A D I A V P L V T K . Y
64 - 81	1838.8872	1837.8799	1837.9534	-40	0 R. A V A E T Q P A Q G E L D A V A R . A
82 - 93	1110.4844	1109.4771	1109.5465	-63	0 R. A T G P A P G P T G E R. E
102 - 126	2436.2502	2435.2430	2435.1136	53	1 R. S G P G P G L G S G S T S G P A D S V M R Q D Y R . A
130 - 140	1381.6244	1380.6171	1380.7044	-63	0 K. V Q R P E P S C R P R . S Carbamidomethyl (C)
141 - 152	1425.7101	1424.7028	1424.6208	58	0 R. S E Y Q P S D A F F E R. E
159 - 167	1157.5535	1156.5462	1156.6142	-59	1 K. D F R A W P L P R . R
214 - 229	1383.6536	1382.6463	1382.6790	-24	0 R. E Q E A P G G A G L A A G K. A
242 - 249	869.4944	868.4872	868.4919	-5	0 K. A G P A W I V R. R
278 - 287	1014.5040	1013.4968	1013.5366	-39	1 R. G R A A D A L N R . Q
330 - 341	1443.6487	1442.6414	1442.6500	-6	0 K. M V H E T S Y S A Q F K. G Oxidation (M)
411 - 424	1460.7675	1459.7602	1459.7154	31	1 K. K S A E G P S T T P D D K . E
425 - 433	1107.5116	1106.5043	1106.5026	2	1 K. E Q S K E M N N K . L
451 - 472	2236.1045	2235.0972	2235.1747	-35	1 K. T Q G P V A T E D K D Q G S V P G L L K. G
462 - 483	2293.0537	2292.0464	2292.2148	-73	1 K. D Q G S V P G L L R G Q G P M V Q P L K. K Oxidation (M)
561 - 571	1235.6193	1234.6120	1234.6670	-45	1 K. D Q G P R I P E P V K . N
572 - 593	2268.0825	2267.0752	2267.1290	-24	1 K. N Q A P M V P A P V K D E G P M V S A S V K. D Oxidation (M)
583 - 604	2261.0647	2260.0574	2260.0715	-6	1 K. D E G P M V S A S V K D Q G P M V S A P V K. D 2 Oxidation (M)
594 - 604	1128.5071	1127.4998	1127.5645	-57	0 K. D Q G P M V S A P V K . D
594 - 615	2246.1941	2245.1868	2245.1777	4	1 K. D Q G P M V S A P V K D Q G P I V P A P V K. G Oxidation (M)
638 - 648	1308.6019	1307.5947	1307.5816	10	0 K. D Q G P V P E H F K. D Oxidation (M)
649 - 659	1149.4705	1148.4632	1148.5383	-65	0 K. D E S A M A T A P I K . N Oxidation (M)
726 - 736	1179.5759	1178.5687	1178.6295	-52	0 K. D Q G P V L Q P F K. N

No match to: 804.0929, 807.3615, 824.4319, 825.0756, 827.4478, 832.4443, 835.0294, 840.4525, 841.4542, 842.5109,

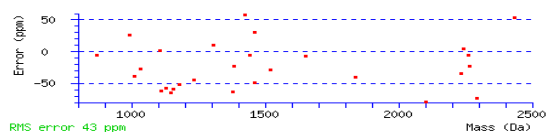


Figure 21. Identification of MAP6 by mascot database search of band 2 (Search 1)

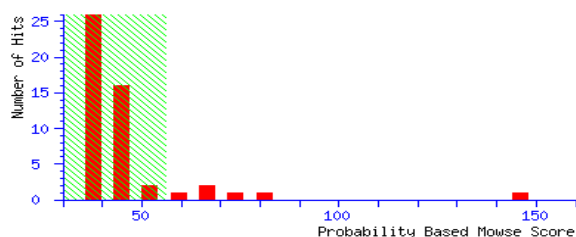
MAP6_HUMAN (Search 2)

{MATRIX} Mascot Search Results *{SCIENCE}*

User : Yumin Song
Email : songyumin00@gmail.com
Search title :
Database : SwissProt 56.9 (412525 sequences; 148809765 residues)
Taxonomy : Homo sapiens (human) (20402 sequences)
Timestamp : 26 Mar 2009 at 20:54:05 GMT
Top Score : 146 for **Mixture 1**, K2C1_HUMAN + K1C10_HUMAN

Probability Based Mowse Score

Protein score is $-10 \cdot \log(P)$, where P is the probability that the observed match is a random event. Protein scores greater than 56 are significant ($p < 0.05$).



Concise Protein Summary Report

Format As [Help](#)
Significance threshold $p <$ Max. number of hits

- Mixture 1** Total score: **146** Expect: $5.1e-11$ Queries matched: 45
Components (only one family member shown for each component):
[K2C1_HUMAN](#) Mass: 65978 Score: **82** Expect: 0.00011 Queries matched: 24
Keratin, type II cytoskeletal 1 OS=Homo sapiens GN=KRT1 PE=1 SV=5
[K1C10_HUMAN](#) Mass: 59475 Score: **76** Expect: 0.00049 Queries matched: 23
Keratin, type I cytoskeletal 10 OS=Homo sapiens GN=KRT10 PE=1 SV=4
- [K2C1_HUMAN](#) Mass: 65978 Score: **82** Expect: 0.00011 Queries matched: 24
Keratin, type II cytoskeletal 1 OS=Homo sapiens GN=KRT1 PE=1 SV=5
- [K1C10_HUMAN](#) Mass: 59475 Score: **76** Expect: 0.00049 Queries matched: 23
Keratin, type I cytoskeletal 10 OS=Homo sapiens GN=KRT10 PE=1 SV=4
- [MAP6_HUMAN](#) Mass: 86452 Score: **67** Expect: 0.0038 Queries matched: 25
Microtubule-associated protein 6 OS=Homo sapiens GN=MAP6 PE=1 SV=2

Search Parameters

Type of search : Peptide Mass Fingerprint
Enzyme : Trypsin
Variable modifications : Carbamidomethyl (C), Oxidation (M)
Mass values : Monoisotopic
Protein Mass : Unrestricted
Peptide Mass Tolerance : ± 100 ppm
Peptide Charge State : 1+
Max Missed Cleavages : 1
Number of queries : 163

MASCOT Mascot Search Results

Protein View

Match to: MAP6_HUMAN Score: 67 Expect: 0.0038
 Microtubule-associated protein 6 OS=Homo sapiens GN=MAP6 PE=1 SV=2

Nominal mass (M_r): 86452; Calculated pI value: 9.20
 NCBI BLAST search of MAP6_HUMAN against nr
 Unformatted [sequence string](#) for pasting into other applications

Taxonomy: [Homo sapiens](#)

Variable modifications: Carbamidomethyl (C), Oxidation (M)
 Cleavage by Trypsin: cuts C-term side of KR unless next residue is P
 Number of mass values searched: 163
 Number of mass values matched: 25
 Sequence Coverage: 37%

Matched peptides shown in **Bold Red**

```

1  MAWPCITRAC  CIARFWNQLD  KADIAVPLVF  TKYSEATEHP  GAPPQPPPPQ
51  QQAQPALAPP  SARAVAIETQ  PAQGELDAVA  RATGPAPGPT  GEREPAAAGPG
101 RSGPGPGLGS  GSTSGPADSV  MRQDYRAWKV  QRPEPSCRPR  SEYQPSDAPF
151 ERETQYQKDF  RAWPLPRRGD  HPWIPKPVQI  SAASQASAPI  LGAPKRRPQS
201 QERWPFVQAAA  EAREQEAAPG  GAGGLAAGKA  SGADERDTRR  KAGPAWIVRR
251 AEGLGHEQTP  LPAAQAQVQA  TGPEAGRGRA  AADALNRQIR  EEVASAVSSS
301 YRNEFRAWTD  IKPVKPIKAK  PQYKPPDDKM  VHETSYSAQF  KGEASKPTTA
351 DNKVIDRRRI  RSLYSEPFKE  PPKVEKPSVQ  SSKPKKTSAS  HKPTRKAKDK
401 QAVSGQAARK  KSABGPSTTK  PDDKEQSKEM  NNNKLAEKES  LAQFVSDSSK
451 TQGPVATEPD  KDQGSVVPGL  LKGQGMVQE  PLKKQGSVVP  GPPKDLGPMI
501 PLPVKDQDHT  VPEPLKNESP  VISAPVKDQG  PSVVPVPPKNQ  SEMVBAKVVD
551 QGSVVPESLK  DQGPRIPEPV  KNQAPMVEAP  VKDEGPMVSA  SVKDQGMVS
601 APVKDQGPVIV  PAPVRGEGPI  VPAPVKDEGP  MVSAPIKDQD  PMVEHPKDE
651 SAMATAPIKN  QGSVMSEPVK  NQGLVVSQEV  KDQDVVVEPH  AKVHDSAVVA
701 PVKNQGPVVP  ESVKNQDPIL  PVLVKDQGET  VLQPPKNQGR  IVPEPLKNQV
751 PIVPVPLKDQ  DPLVEVPAKD  QGPAVPEPLK  TQGPRDPQLP  TVSEPLRVMI
801 PTAPHTIEYE  SSP
  
```

Show predicted peptides also

Sort Peptides By Residue Number Increasing Mass Decreasing Mass

Start - End	Observed	Mr (expt)	Mr (calc)	ppm	Miss	Sequence
1 - 8	993.5037	992.4964	992.4572	39	0	--MAWPCITR.A Oxidation (M)
1 - 8	1034.4652	1033.4579	1033.4837	-25	0	--MAWPCITR.A Carbamidomethyl (C)
2 - 14	1463.6091	1462.6019	1462.6995	-67	1	M.AWPCITRACCIAR.F
15 - 32	2104.9741	2103.9668	2104.1357	-80	1	R.FWNQLDKADIAVPLVFTK.Y
82 - 93	1110.4933	1109.4860	1109.5465	-55	0	R.ATGPAPGPTGER.E
102 - 126	2436.2546	2435.2474	2435.1136	55	1	R.SGPGPGLSGSTSGPADSVMRQDYR.A
130 - 140	1381.6506	1380.6434	1380.7044	-44	0	K.VQRPPEPSCRPR.S Carbamidomethyl (C)
141 - 152	1425.7361	1424.7288	1424.6208	76	0	R.SEYQPSDAPFER.E
214 - 229	1383.6750	1382.6678	1382.6790	-8	0	R.EQEAAPGGAGGLAAGK.A
278 - 287	1014.5063	1013.4990	1013.5366	-37	1	R.GRAAADALNR.Q
330 - 341	1427.8041	1426.7968	1426.6551	99	0	K.MVHETSYSAQFK.G
411 - 424	1460.7634	1459.7562	1459.7154	28	1	K.KSABGPSTTKPDDK.E
425 - 433	1107.5181	1106.5108	1106.5026	7	1	K.EQSKEMNNK.L
451 - 472	2236.0681	2235.0608	2235.1747	-51	1	K.TQGPVATEPDKDQGSVVPGLLK.G
462 - 483	2293.0503	2292.0430	2292.2148	-75	1	K.DQGSVVPGLLKQGMVQEPLK.K Oxidation (M)
517 - 527	1140.5328	1139.5256	1139.6186	-82	0	K.NESFVISAPVK.D
528 - 538	1120.5282	1119.5209	1119.5924	-64	0	K.DQGPSVVPVPPK.N
550 - 560	1158.5483	1157.5411	1157.5928	-45	0	K.DQGSVVPESLK.D
583 - 604	2261.0837	2260.0765	2260.0715	2	1	K.DEGPMVSAVVKDQGMVSAVVK.D 2 Oxidation (M)
594 - 604	1128.5109	1127.5036	1127.5645	-54	0	K.DQGMVSAVVK.D
594 - 615	2246.2129	2245.2056	2245.1777	12	1	K.DQGMVSAVVKDQGPVIVPAPVK.G Oxidation (M)
649 - 659	1149.4845	1148.4772	1148.5383	-53	0	K.DESAMATAPIK.N Oxidation (M)
649 - 670	2290.0269	2289.0196	2289.0981	-34	1	K.DESAMATAPIKNQGSVMSEPVK.N
671 - 692	2315.1653	2314.1580	2314.2281	-30	1	K.NQGLVVSQEVKQDVVVEPHAK.V
726 - 736	1179.5774	1178.5701	1178.6295	-50	0	K.DQGPVTLQPPK.N

No match to: 804.1010, 807.3674, 825.0730, 825.4619, 827.4537, 832.4532, 835.0400, 840.4608, 841.4635, 842.5103,

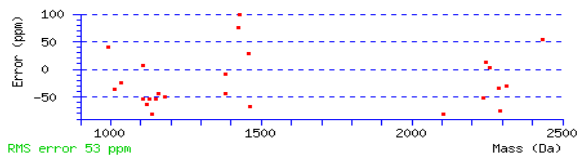


Figure 22. Identification of MAP6 by mascot database search of band 2 (Search 2)

BIBLIOGRAPHY

1. World Health Organization International Agency for Research on Cancer (June 2003). "World Cancer Report". Retrieved on 2009-03-26.
<http://www.iarc.fr/en/Publications/PDFs-online/World-Cancer-Report/World-Cancer-Report>.
2. World Health Organization (February 2006). "Fact sheet No. 297: Cancer".
<http://www.who.int/mediacentre/factsheets/fs297/en/index.html>. Retrieved on 2009-03-26.
3. http://www.breastcancer.org/symptoms/understand_bc/statistics.jsp
4. Rowinsky, E. K., et al., Taxol: the first of the taxanes, an important new class of antitumor agents. *Semin Oncol*, 1992. 19(6): 646-62
5. George A Orr, Pascal Verdier-Pinard, Hayley McDaid1 and Susan Band Horwitz. Mechanisms of Taxol resistance related to microtubules. *Oncogene* (2003) 22, 7280–7295
6. Alexandre Maucuer, Jacques H. Camonis and André Sobel; Stathmin Interaction with a Putative Kinase and Coiled-Coil-Forming Protein Domains; *Proceedings of the National Academy of Sciences of the United States of America*, Vol. 92, No. 8 (Apr. 11, 1995), pp. 3100-3104
7. Marc R. Wilkins, Christian Pasquali, Ron D. Appel, Keli Ou, Olivier Golaz, Jean-Charles Sanchez, Jun X. Yan, Andrew. A. Gooley, Graham Hughes, Ian Humphery-Smith, Keith L. Williams & Denis F. Hochstrasser (1996). "From Proteins to Proteomes: Large Scale Protein Identification by Two-Dimensional Electrophoresis and Arnino Acid Analysis". *Nature Biotechnology* 14 (1): 61–65.
8. UNSW Staff Bio: Professor Marc Wilkins;
<http://www.babs.unsw.edu.au/directory.php?personnelID=12>

9. Simon Rogers, Mark Girolami, Walter Kolch, Katrina M. Waters, Tao Liu, Brian Thrall and H. Steven Wiley (2008). "Investigating the correspondence between transcriptomic and proteomic expression profiles using coupled cluster models". *Bioinformatics* 24 (24): 2894–2900
10. Vikas Dhingraa, Mukta Gupta, Tracy Andacht and Zhen F. Fu (2005). "New frontiers in proteomics research: A perspective". *International Journal of Pharmaceutics* 299 (1–2): 1–18.
11. Buckingham, Steven (5 2003). "The major world of microRNAs".
<http://www.nature.com/horizon/rna/background/micrnas.html>. Retrieved on 2009-01-14
12. Drews O, Zong C, Ping P. Exploring proteasome complexes by proteomic approaches. *Proteomics*. 2007 Apr;7 (7):1047-58
13. Geoffrey M. Cooper; *The Cell A Molecular Approach; Cell Structure and Function - Cytoskeleton and Cell Movement*;
<http://www.ncbi.nlm.nih.gov/books/bv.fcgi?indexed=google&rid=cooper.section.1820>
14. Mollinedo, F., Gajate, C., Microtubules, microtubule-interfering agents and apoptosis. *Apoptosis*, 2003. 8(5): 413-50
15. Mitchison, T. J., Kirschner, M., Dynamic instability of microtubule growth. *Nature*, 1984. 312: 237-42
16. Microtubule - Definitions from Dictionary.com". dictionary.reference.com.
<http://dictionary.reference.com/browse/Microtubule>. Retrieved on 2008-05-15
17. Kumar, N. Taxol-induced polymerization of purified tubulin. Mechanism of action. *J Biol Chem*, 1981. 256: 10435-41
18. Jordan, M. A., Mechanism of action of antitumor drugs that interact with microtubules and tubulin. *Curr Med Chem Anti-Canc Agents*, 2002. 2: 1-17
19. Derry, W., Wilson, L., Jordan, M. A., Substoichiometric binding of Taxol suppresses

microtubule dynamics. *Biochemistry*, 1995. 34: 2203-11

20. Goodman and Walsh, p51
21. Khayat, D., Antoine, E. C., Coeffic, D., Taxol in the management of cancers of the breast and the ovary. *Cancer Invest*, 2000. 18: 242-60
22. Schiff, P. B., Horwitz, S. B., Taxol stabilizes microtubules in mouse fibroblast cells. *Proc Natl Acad Sci USA*, 1980. 77: 1561-65
23. Cardone L, de Cristofaro T, Affaitati A, Garbi C, Ginsberg MD, Saviano M, Varrone S, Rubin CS, Gottesman ME, Avvedimento EV, Feliciello A. A-kinase anchor protein 84/121 are targeted to mitochondria and mitotic spindles by overlapping amino-terminal motifs. *J Mol Biol*. 2002 Jul 12;320(3):663-75
24. Jordan MA, Wilson L. Microtubules and actin filaments: dynamic targets for cancer chemotherapy. *Curr Opin Cell Biol*. 1998 Feb;10(1):123-30.
25. DiPaolo, G., et al. Phosphorylation regulates the microtubule-destabilizing activity of stathmin and its interaction with tubulin. *FEBS Lett*, 1997. 416: 149-52
26. Larsson, N., et al. Control of microtubule dynamics by oncoprotein 18: dissection of the regulatory role of multisite phosphorylation during mitosis. *Mol Cell Biol*, 1997: 5530-39
27. Mistry, S. J. and Atweh, G. F., Role of stathmin in the regulation of the mitotic spindle: potential applications in cancer therapy. *Mount Sinai J Med*, 2002. 69(5): 299-304
28. Larsson N, Segerman B, Gradin HM, Wandzioch E, Cassimeris L, Gullberg M. Mutations of oncoprotein 18/stathmin identify tubulin-directed regulatory activities distinct from tubulin association. *Mol Cell Biol*. 1999 Mar;19(3):2242-50
29. Hanash SM, Strahler JR, Kuick R, Chu EH, Nichols D. Identification of a polypeptide associated with the malignant phenotype in acute leukemia. *J Biol Chem*. 1988 Sep 15;263(26):12813-5

30. Nylander K, Marklund U, Brattsand G, Gullberg M, Roos G. Immunohistochemical detection of oncoprotein 18 (Op18) in malignant lymphomas. *Histochem J*. 1995 Feb;27(2):155-60.
31. Bièche I, Lachkar S, Becette V, Cifuentes-Diaz C, Sobel A, Lidereau R, Curmi PA. Overexpression of the stathmin gene in a subset of human breast cancer. *Br J Cancer*. 1998 Sep;78(6):701-9
32. Curmi PA, Noguès C, Lachkar S, Carelle N, Gonthier MP, Sobel A, Lidereau R, Bièche I. Overexpression of stathmin in breast carcinomas points out to highly proliferative tumours. *Br J Cancer*. 2000 Jan;82(1):142-50.
33. Gonçalves A, Braguer D, Kamath K, Martello L, Briand C, Horwitz S, Wilson L, Jordan MA. Resistance to Taxol in lung cancer cells associated with increased microtubule dynamics. *Proc Natl Acad Sci U S A*. 2001 Sep 25;98(20):11737-42. Epub 2001 Sep 18.
34. Shevchenko A, Tomas H, Havlis J, Olsen JV, Mann M. In-gel digestion for mass spectrometric characterization of proteins and proteomes. *Nat Protoc*. 2006;1(6):2856-60
35. Roepstorff, P., Mass spectrometry in protein studies from genome to function. *Curr Opin Biotechnol*, 1997. 8(1): 6-13
36. Karas, M. and F. Hillenkamp, Laser desorption ionization of proteins with molecular masses exceeding 10,000 daltons. *Anal Chem*, 1988. 60(20): 2299-301
37. Pappin, D. J., P. Hojrup, and A.J. Bleasby, Rapid identification of proteins by peptidemass fingerprinting. *Curr Biol*, 1993. 3(6): 327-32
38. Yang Y, Thannhauser TW, Li L, Zhang S. Development of an integrated approach for evaluation of 2-D gel image analysis: impact of multiple proteins in single spots on comparative proteomics in conventional 2-D gel/MALDI workflow. *Electrophoresis*. 2007 Jun;28(12):2080-94
39. Berth M, Moser FM, Kolbe M, Bernhardt J. The state of the art in the analysis of two-dimensional gel electrophoresis images. *Appl Microbiol Biotechnol*. 2007 Oct;76(6):1223-43. Epub 2007 Aug 23

40. Mann M, Hendrickson RC, Pandey A. Analysis of proteins and proteomes by mass spectrometry. *Annu Rev Biochem.* 2001;70:437-73
41. King R, Bonfiglio R, Fernandez-Metzler C, Miller-Stein C, Olah T. Mechanistic investigation of ionization suppression in electrospray ionization. *J Am Soc Mass Spectrom* 2000;11:942–50
42. Thomas M. Annesley; Ion Suppression in Mass Spectrometry; *Clinical Chemistry* 49:7 1041 - 1044 (2003)
43. Beavis, R. C. (1992). " α -Cyano-4-hydroxycinnamic acid as a matrix for matrix-assisted laser desorption mass spectrometry". *Org. Mass Spectrom.* 27: 156–8
44. Unlu, M., Morgan, M. E., Minden, J.S., Difference gel electrophoresis: a single gel method for detecting changes in cell extracts. *Electrophoresis*, 1997. 18: 2071-2077
45. Timms JF, Cramer R. Difference gel electrophoresis. *Proteomics.* 2008 Dec;8(23-24):4886-97
46. Minden J. Comparative proteomics and difference gel electrophoresis. *Biotechniques.* 2007 Dec;43(6):739, 741, 743
47. Ishihama Y, Rappsilber J, Mann M. Modular stop and go extraction tips with stacked disks for parallel and multidimensional Peptide fractionation in proteomics. *J Proteome Res.* 2006 Apr;5(4):988-94
48. Rappsilber J, Mann M, Ishihama Y. Protocol for micro-purification, enrichment, pre-fractionation and storage of peptides for proteomics using StageTips. *Nat Protoc.* 2007;2(8):1896-906
49. Rappsilber J, Ishihama Y, Mann M. Stop and go extraction tips for matrix-assisted laser desorption/ionization, nanoelectrospray, and LC/MS sample pretreatment in proteomics. *Anal Chem.* 2003 Feb 1;75(3):663-70
50. Arash Nakhost, Nurul Kabir, Paul Forscher, and Wayne S. Sossin; Protein Kinase C Isoforms Are Translocated to Microtubules in Neurons; *J. Biol. Chem.*, Vol. 277, Issue 43,

40633-40639

51. R Prekeris, MW Mayhew, JB Cooper and DM Terrian. Identification and localization of an actin-binding motif that is unique to the epsilon isoform of protein kinase C and participates in the regulation of synaptic function. *The Journal of Cell Biology*, Vol 132, 77-90
52. Bae KM, Wang H, Jiang G, Chen MG, Lu L, Xiao L. Protein kinase C epsilon is overexpressed in primary human non-small cell lung cancers and functionally required for proliferation of non-small cell lung cancer cells in a p21/Cip1-dependent manner. *Cancer Res.* 2007 Jul 1;67(13):6053-63
53. McJilton MA, Van Sikes C, Wescott GG, Wu D, Foreman TL, Gregory CW, Weidner DA, Harris Ford O, Morgan Lasater A, Mohler JL, Terrian DM. Protein kinase Cepsilon interacts with Bax and promotes survival of human prostate cancer cells. *Oncogene.* 2003 Sep 11;22(39):7958-68
54. Lu D, Huang J, Basu A. Protein kinase Cepsilon activates protein kinase B/Akt via DNA-PK to protect against tumor necrosis factor-alpha-induced cell death. 1: *J Biol Chem.* 2006 Aug 11;281(32):22799-807
55. Nogales E. Structural insights into microtubule function. *Annu Rev Biochem.* 2000;69:277-302
56. Ookata, K., et al., Cyclin B interaction with microtubule-associated protein 4 (MAP4) targets p34cdc2 kinase to microtubules and is a potential regulator of M-phase microtubule dynamics. *J Cell Biol*, 1995. 128(5): 849-62
57. Cassimeris L. The oncoprotein 18/stathmin family of microtubule destabilizers. *Curr Opin Cell Biol.* 2002 Feb;14(1):18-24
58. Murphy M, Hinman A, Levine AJ. Wild-type p53 negatively regulates the expression of a microtubule-associated protein. *Genes Dev.* 1996 Dec 1;10(23):2971-80
59. Bosc C, Cronk JD, Pirollet F, et al. (1996). "Cloning, expression, and properties of the microtubule-stabilizing protein STOP." *Proc. Natl. Acad. Sci. U.S.A.* 93 (5): 2125-30